Title
THE DECAYS OF 176Ta, 1T6Lu AND ^6m Lu TO LEVELS IN ' Hf

Authors
Bernthal, F.M.
Rasmussen, J.O.
Hollander, J.M.

Publication Date
1970-04-01

Submitted to Physical Review

UCRL-19587
Preprint

c. 2

THE DECAYS OF ^{176}Ta, ^{176}Lu AND ^{176m}Lu TO LEVELS IN ^{176}Hf

F. M. Bernthal, J. O. Rasmussen, and J. M. Hollander

April 1970

AEC Contract No. W-7405-eng-48

LAWRENCE RADIATION LABORATORY
UNIVERSITY of CALIFORNIA BERKELEY

34

DISCLAIMER

THE DECAYS OF ^{176}Ta, ^{176}Lu AND ^{176m}Lu TO LEVELS IN ^{176}Hf

F. M. Bernthal and J. O. Rasmussen

Lawrence Radiation Laboratory
University of California
Berkeley, California 94720

and

Yale University
New Haven, Connecticut 06520

and

J. M. Hollander

Lawrence Radiation Laboratory
University of California
Berkeley, California 94720

April 1970

ABSTRACT

The locations of 48 energy levels in ^{176}Hf have been deduced from γ-ray singles, conversion-electron, and γ-γ coincidence measurements on the EC-β^+ decay of ^{176}Ta. Over 300 γ-ray transitions have been observed in the ^{176}Ta decay spectrum, and about 140 of these have been definitely assigned to the ^{176}Hf level scheme on the basis of 75 γ-γ coincidence spectra. Spin and parity assignments are proposed for 27 levels besides the ground-state rotational band members. Less extensive γ-ray singles data from ^{176}Lu and ^{176m}Lu decay have also been obtained; these are found to be consistent with the ^{176}Hf level structure proposed on the basis of ^{176}Ta decay data. Two 0^+ excitations in ^{176}Hf identified at 1150 and 1293 keV are found to display quite different decay properties. Evidence for the existence of a series of low-spin four-quasiparticle states near 3 MeV is cited. The ^{176}Hf level structure is compared with available theoretical calculations, and a preliminary interpretation of several unusual features of the level scheme is presented.

I. INTRODUCTION

One of the most complicated radioactive decay processes yet studied is that associated with the EC-β^+ decay of 8-hour ^{176}Ta to levels in ^{176}Hf. The complexity of this decay was early encountered by Rasmussen and Shirley[1] and was also witnessed in the electron study by Harmatz et al.[2] Attempts to construct a decay scheme at that time, and subsequently with use of NaI(TI) scintillation detectors were largely unsuccessful.[3,4]

Although high-resolution Ge(Li) detection systems have revealed the intricacies of many complex γ-ray spectra, the elucidation of decay schemes of nuclei such as ^{176}Ta has until recently remained a formidable task. With the introduction of on-line computers and associated multiparameter data acquisition systems however, the detailed study of even the most complex decay schemes is now possible.

In this paper, we report the results of γ-ray singles, γ-γ coincidence, and conversion-electron spectroscopic studies carried out on the decays of ^{176}Ta, ^{176}Lu, and ^{176m}Lu to levels in ^{176}Hf. On the basis of these data, we have constructed a level scheme for the nucleus ^{176}Hf consisting of 48 excited states. About 140 transitions have been assigned to the level scheme on the basis of the ^{176}Ta γ-γ coincidence data. Much less extensive ^{176m}Lu decay data which we have obtained support the ^{176}Ta assignments. Two low-lying excited 0^+ states displaying markedly different decay characteristics have been identified in ^{176}Hf. Evidence for a series of high-energy, low-spin four-quasiparticle states is also reported, and the even-spin members of the $K = 0^-$ "octupole vibrational" band are thought to be identified.

II. EXPERIMENTAL

A. Target and Source Preparation

Sources of ^{176}Ta were prepared via the ^{175}Lu (α, 3n) ^{176}Ta reaction by irradiating $\approx$ 35 mg samples of 99.94% enriched $^{175}Lu_2O_3$ at the LRL 88-inch cyclotron with 38 MeV alpha particles. Two-hour irradiations at about 18μA beam current produced an estimated 10 mCi ^{176}Ta activity for each experiment.

The Ta activity was separated from other reaction products by extraction from 6N HCl solution using 2, 4-dimethyl--3-pentanone (diisopropyl ketone), a procedure described in Ref. 5. The γ-ray counting sources were prepared on aluminum or Teflon backings by evaporating to dryness small quantities of the extracted carrier-free Ta in water solution. Electron sources were similarly prepared by liquid deposition of the activity onto 0.25-mil gold-anodized mylar.

Counting was usually begun within three hours after the end of irradiation. Relatively small quantities of ^{175}Ta, ^{177}Ta, and ^{178}Ta contamination were noted in the γ-ray spectra.

B. Experimental Apparatus

A variety of detection systems was used in this study to make measurements of: a) the singles γ-ray spectrum; b) the conversion-electron spectrum; c) the γ-ray "pair" spectrum; d) the entire γ-γ coincidence spectrum of ^{176}Ta decay.

The γ-ray singles spectrum of ^{176}Ta was investigated with use of 1) a 10-cm^3 planar Ge(Li) detector with resolution (FWMH) 2.3 keV at 1.17 MeV; 2) a 1-cm^3 "thin-window" Ge(Li) detector with resolution 0.8 keV at 122 keV; 3) a 7-cm^3 planar Ge(Li) detector with resolution 2.1 keV at 1.17 MeV, a component of the Compton-suppression system at LRL, Livermore.[6]

The electron spectrum was obtained with a 3-mm deep by 1-cm^2 Si(Li) diode operated at a bias of 650V and a temperature of 110°K. The resolution of this system was about 2.5 keV FWHM for the 1.06 MeV ^{207}Bi K-conversion electron line.

Some additional information on the high-energy photon emission spectrum from ^{176}Ta decay was provided by the "pair" or "double-escape peak" spectrum, obtained with a 5-crystal Ge(Li)-NaI(Tl) pair spectrometer. This apparatus features a split NaI(Tl) annulus consisting of four optically isolated sections that surround a 10 cm^3 planar Ge(Li) detector (resolution 2.0 keV).

With the exception of the Compton-suppressed data (taken with a Nuclear Data Model 161-F 4096-channel analyzer), nearly all of the singles γ-ray and electron spectra were gathered with a PDP-7 computer used "on-line" as a pulse height analyzer. For the acquisition of γ-γ coincidence data, we employed two Ge(Li) detectors, 35 cm^3 and 10 cm^3 in volume, together with a multiparameter data acquisition system designed, built, and interfaced to the PDP-7 by Robinson *et al.*[7] With this system all of the γ-γ coincidence data, together with their timing distributions, could be digitized and stored serially on IBM standard magnetic tape for later analysis with the LRL CDC-6600 computer. A detailed description of the various detection systems and associated electronics employed in this study may be found in Ref. 8.

C. Experimental Results

1. The ^{176}Ta γ-ray Spectrum

The Compton-suppressed singles γ-ray spectrum from the decay of ^{176}Ta has allowed us to identify over 300 transitions associated with the energy levels in ^{176}Hf. Although many of the transitions observed were weak, the interfering

activities from ^{178}Ta, ^{177}Ta, ^{175}Ta, and its daughter, ^{175}Hf were also found to be relatively weak, and in any case none of these nuclei has lines of significant intensity at energies above ≈ 1 MeV. Figures 1 and 2 show the γ-ray singles spectrum obtained with the Livermore Compton-suppression spectrometer. The data shown represent the results from two separate runs: one from 75 to 1250 keV, the other a high-energy run from 1.06 to 3.00 MeV. The lines from ^{175}Ta, ^{177}Ta, ^{178}Ta, and ^{175}Hf contamination are so identified.

One does not normally expect to see escape peaks appearing prominently in a Compton-suppressed spectrum, since single-escape peaks are presumably suppressed as efficiently as are Compton scattered events, while the double escape lines are even further suppressed. Accordingly, escape peaks found in the low energy spectrum are at most very weak (Fig. 1). Comparison of the background region around 1200 keV in Figs. 1 and 2 reveals unfortunately that the Compton-suppression anti-coincidence unit was operating intermittently during the high energy run; consequently the strong double-escape lines from the 2832- and 2920-keV transitions are still prominent in Fig. 2. We did not retake these data, however, since the "pair" spectrum served to resolve any ambiguities in the high-energy portion of the ^{176}Ta singles spectrum. The pair spectrum (Ref. 8) displays resolution appreciably better than in Fig. 2, and although the statistics are poorer by a factor of four, the peak-to-background ratio from about 1600 to 2700 keV is also more favorable than in the singles spectrum.

In column 1 of Tables I (a and b) we list all the γ-rays observed from the decay of ^{176}Ta. We have chosen to classify the γ-rays into two categories depending on their intensity. In Table I-a are listed only the lines with intensity ≥ 1% relative to the 710.5-keV line. Table I-b lists those lines with

intensity < 1% of the 710-keV intensity. With few exceptions, we have been unable to place definitely in the decay scheme any of the transitions in the latter category. Though we believe the energies of the stronger lines to be precise to 0.2 keV or better over the entire energy range of the spectrum[†], we have not considered simple energy sums and differences alone to provide sufficient information for definite placement of a transition in the level scheme, because of the very high density of lines. Moreover, as a consequence of the ease with which coincidence data can now be gathered by use of multiparameter data systems similar to that employed in this work, it is not unreasonable (and in the case of ^{176}Ta it seems necessary) to require coincidence confirmation of all assignments to a proposed level scheme.

Accordingly, we have gathered extensive γ-γ coincidence information on the ^{176}Ta decay. Because of the complexity and bulk of these data (about 75 separate coincidence spectra have been sorted and analyzed for peak energies and intensities), it is not possible to display here all of the spectra, or even to provide a meaningful "coincidence matrix" reduction of the data. We therefore reproduce only a few of the coincidence spectra that are of particular interest and refer the reader to Ref. 8 for a complete catalogue of the data. Figures 3 show the coincidence spectra for the two ^{176}Hf ground-rotational-band transitions observed at 88 and 202 keV. Subtraction of background and random events has been carried out by the computer code during the sorting process, so that the spectra shown presumably represent only "valid" photopeak coincidences. The FWHM resolving time of the coincidence time-amplitude curve was 24 nsec.

[†]The γ-ray spectrometers were calibrated for energy with use of the standards listed in Ref. 8. In the high-energy region of the spectrum we have relied heavily upon the recent ^{56}Co standardization work by Gunnink, et al.[9]

Digital time gates of 65 nsec were set on this curve for the purpose of sorting prompt and random events.

In Fig. 4 we display three additional coincidence spectra of particular importance to the interpretation of the ^{176}Ta decay data. The three spectra were obtained by setting adjacent digital windows at 1155, 1157, and 1159 keV on the strong γ-ray multiplet appearing at about 1159 keV in the ^{176}Ta singles spectrum. The relative intensities of the various lines in the coincidence spectra clearly indicate the complexity of the region in question.

By making full use of the 4096 × 4096 × 512-channel matrix of γ-ray energy vs. time coincidence information provided by the multiparameter system used in this study, it is in principle possible to extract lifetime data for isomeric states appearing in the decay in question, but the low spin of the parent nucleus makes it seem unlikely that isomers of lifetime sufficiently long for measurement by our apparatus would be appreciably populated by ^{176}Ta decay.

2. The ^{176}Ta Conversion Electron Spectrum

In Figs. 5 and 6 we show portions of the conversion electron data gathered with the 3 mm × 1 cm^2 Si(Li) detector. Figure 5 displays the low energy conversion spectrum from 160 to 1600 keV. Figure 6 shows the high-energy (1.0 to 3.0 MeV) electron spectrum. An interesting aspect of the latter spectrum is the appearance of the 2920.4- and 2832.0-keV photon double-escape peaks, a feature one does not usually see in Si(Li) spectra.

In Table II we list the conversion electron lines observed from the decay of ^{176}Ta. Because the electron detection efficiency of the Si(Li) crystal is poorly known above 1.6 MeV, the relative intensity errors indicated reflect the large uncertainty associated with extrapolating the Si(Li) efficiency curve to

3.0 MeV.[8] Most of the transitions in the ^{176}Ta spectrum are M1, E2, mixed M1-E2, or E1-M2 in character. (As expected, there is little population of states having more than 3 units of angular momentum, with the exception of the 4+ member of the ground band.) Only minimal information on transition multipolarity can be gleaned from K-conversion coefficients alone in such cases, and the complexity of the ^{176}Ta spectrum seriously limits the usefulness of the Si(Li) conversion data.

We have included in Table I whatever unambiguous information was provided by the Si(Li) electron spectrum. Conversion coefficients were determined by normalization to the theoretical conversion coefficient of the presumably pure E2 ground rotational band transition at 202 keV with use of the tables of Hager and Seltzer.[10] In the low-energy region of the electron spectrum where the permanent magnet spectrograph results of Harmatz et al.[2] provide more definitive information, we list those data.

D. Proposed ^{176}Hf Level Scheme

1. Data Analysis and Construction of the Level Scheme

In Fig. 7 we show schematically the decay of ^{176}Ta to levels in ^{176}Hf as derived from our data. On the basis of coincidence, singles γ-ray, and conversion-electron data we have placed in the level scheme essentially all transitions with intensity $\geq 4\%$ of the 710.5-keV photon intensity. The transitions placed in Fig. 7 represent only those lines for which definite assignments could be made on the basis of γ-γ coincidence data. There are, however, numerous weak lines which can be placed on the basis of energy data alone, and undoubtedly some of those assignments are correct. Therefore in Fig. 8 we show

again the ^{176}Hf level scheme, here indicating the transitions from ^{176}Ta decay which we were able to fit into the established levels (those of Fig. 7) on the basis of energy information. We also show a few low energy transitions (dashed lines) whose presence is indicated by coincidence data, but which were not observed in either the photon or electron spectrum.

A detailed exposition on the assignment of each transition to its place in the level scheme seems impractical, and in any case all of the γ-γ coincidence data are available in Ref. 8. We do, however, wish to comment on a few points of particular interest and importance to the construction of the level scheme.

a. The 1159-keV multiplet. The strong "line" at 1159-keV has consistently plagued all previous attempts to interpret the decay of ^{176}Ta.† On the basis of centroid shifts in coincidence data we have confirmed that this "line" is in fact a triplet of close-lying lines arranged in such a way as to make them extremely difficult to detect in γ-ray singles data displaying resolution poorer than about 3 keV at ^{60}Co. Analysis of the three spectra coincident with the 466-, 710-, and 1023-keV transitions revealed the following:

Gate line (keV)	"1159"-keV centroid location (channel)	Centroid energy (keV)
466.2	1469.3	1155.2 ± 0.2
1023.1	1472.2	1157.6 ± 0.2
710.5	1474.6	1159.4 ± 0.1

†Cf. for example the independent Ge(Li) work on ^{176}Ta decay just published by Boddendijk, et al.[11] These authors also concluded that the 1159-keV peak was complex, but did not make unambiguous assignments of its components to the level scheme.

Consideration of the Compton-suppressed singles data in this region (Fig. 1) would certainly suggest that the line is a doublet, but the singles intensity ratios I_{1155}: I_{1157}: I_{1159} = 12:63:458 make it extremely difficult to detect visually the presence of a third line. With use of experimental peak shape parameters obtained from strong "clean" singlets in the spectrum, however, the computer-generated resolution of the 1159-keV multiplet clearly shows the presence of three peaks. The three coincidence gates set on the multiplet confirm the singles analysis, as can be seen from the 1155-, 1157-, and 1159-keV coincidence spectra in Fig. 4. Finally, the pair spectrum (Ref. 8) clearly shows the 1157-keV component, and indicates its intensity is 13.3% that of the 1159-keV line, in excellent agreement with the 13.7% value obtained from singles data.

b. The 1224-keV γ-ray multiplet. At 1224 keV the presence of complex structure is evident. However, attempts to analyze this group as a doublet indicated the presence also of a high-energy shoulder with energy 1226.8 keV and ≈ 7% of the 1225-keV line intensity. This fact, coupled with rather tenuous evidence from the 1694-keV coincidence spectrum, seemed to justify assignment of the 1226.8-keV transition from the level of that energy to ground. Such an assignment is consistent with the 2+ spin and parity proposed on the basis of K-conversion electron data for the 936- and 1138-keV transitions. Figure 9 compares the doublet and triplet analyses of the complex at 1224-keV. The ^{176m}Lu decay data later confirmed the presence of a line at 1226.6-keV, and verified the computer analysis of the ^{176}Ta data.

c. The low energy transition at 91.2-keV. We find evidence for the presence of a 91.2-keV transition in the "thin-window" high resolution γ-ray spectrum (Fig. 10). Harmatz et al.[2] reported the line in their conversion-electron study, and indicated a likely E2(+M1) multipolarity. There is further

evidence for its presence in our coincidence spectra. The 1066-keV coincidence spectrum[8] clearly shows the 1225-keV line in coincidence, as well as some indication of the weaker 1023-keV line. These data suggest the presence of a transition, unseen in the coincidence spectrum, leading from the 1404.6- to the 1313.3-keV level. This analysis is corroborated by the 1023-keV coincidence spectrum showing the same 1066-keV transition. In this instance, then, we can argue convincingly for the presence of a transition on the basis of coincidence data alone. A similar argument can be constructed to support the proposed presence of a 65.7-keV transition, unobserved in the singles spectrum but presumed to de-excite the 1313-keV level.

d. Complex regions in the ^{176}Ta γ-ray spectrum. Despite the powerful assistance in spectrum analysis afforded by the on-line computer, there remain regions of the ^{176}Ta γ-ray spectrum that have yielded neither to intensive coincidence nor singles studies. Aside from the obvious limitation imposed by detector system resolution, further practical limitations arise from computer memory capacity. The dimensions of our peak analysis program presently allow us to handle multiplets containing up to only six components.

Several regions in the ^{176}Ta γ-ray spectrum require further study with improved resolution:

(1) The region from 508 to 521 keV is quite complex, and the analysis is further complicated by the presence of the broad 511-keV annihilation peak. In addition to the apparently single lines at 508 and perhaps at 512 keV, it appears certain that there are at least three components at 519.7, 521.3, and 521.6 keV in the multiplet. Transitions of those energies have been assigned to the level scheme. There may also be additional components at ≈ 512, 517, and 521 keV.

(2) The (541-547)-keV region is also complex. Coincidence data allow us to place two transitions at 543.2 and 546.5 keV with some confidence, and a third at 540.3 keV with less certainty. It appears from analysis of singles data that there are at least five lines present in this group.

(3) The complexity of the region from 1600 to 1645 keV is evident from Fig. 2. At least eleven lines appear to be present, seven of which are assigned to the level scheme on the basis of coincidence data.

(4) It is not clear how many peaks are "buried" in the low-energy side of the strong doublet at 2832.0 and 2920.4 keV. We suspect there are lines at 2823.6 and 2912.3 keV, but the intensity of each of these is only about 1% that of the neighboring strong line.

e. The 1149.9- and 1293.2-keV E0 transitions. The conversion electron spectrum (Fig. 5) reveals the presence of two lines that have no counterpart in the photon spectrum. These transitions, at 1149.9 and 1293.2 keV, presumably arise from pure E0 conversion processes, and reveal the presence of two low-lying 0+ states in the ^{176}Hf level scheme. Of particular interest and importance is the analysis of the electron data in the 1290-keV region (Fig. 11), for reasons that are discussed in a later section. Based on the analysis shown in Fig. 11, we propose an E0 component in the 1291.0 K-conversion line.

f. The 1224-keV K-Conversion line. It is apparent from even qualitative visual inspection of Fig. 5 that the ratio of intensity of the 1224-keV conversion electron group to that of the 1159-keV group is much larger than the corresponding γ-ray intensity ratio (Fig. 1). Some of the difference might be supposed to arise from the very strong 1159-keV 2- → 2+ transition, presumably E1 in character. However, this E1 transition is once K-forbidden, and

appears to have substantial M2 mixing. One finds then that the 1223-keV transition exhibits a K-conversion coefficient of ≈ 0.035, far too large even for a pure M2 transition (see Fig. 12). But the question of whether the apparently high intensities of both the 1223- and 1291-keV K-conversion lines may be spurious must be considered. The circumstance that the strong groups at 1158-, 1224-, and 1292-keV happen to be separated by about 65 keV (the K-shell electron binding energy) raises the possibility that some of the 1223- and 1291-keV K-electron intensity may be due to x-ray summing with the strong lines from the 1158- and 1224-keV groups, respectively. We believe that this is not the case, however, for the following reasons: (1) There is no evidence for summing effects having distorted the K:L:(M+N) conversion ratio for the strong 710-keV transition in the electron spectrum, where all three groups are cleanly resolved; (2) The relative intensity ratios measured by Harmatz et al.,[2] Boddendijk et al.,[11] and by us for the 1158-, 1224-, and 1292-keV conversion-electron groups are in excellent agreement. These ratios are respectively 1.0:0.9:1.1, 1.0:0.9:1.1, and 1.0:0.9:1.2. (3) In our experimental apparatus, the electron source was positioned about 3 cm from the Si(Li) detector. The detector was mounted on an aluminum annulus of about 1 cm inner diameter to provide both collimation and electrical contact. Thus the solid angle for all our electron spectra was only about 0.7%, so that summing should not be significant.

2. EC-β^+ Decay and Q-Value of ^{176}Ta

There has been some disagreement on the question of the Q-value for EC-β^+ decay of ^{176}Ta to ^{176}Hf. The NDS estimate for the ^{176}Ta decay energy, taken from β-decay systematics, is 3.2 MeV,[12] and the recent calculations of

Garvey et al. suggest Q_{EC} = 3.02 MeV.[13] However, Fominikh et al.[14] reported a (3000 ± 80) keV component in the ^{176}Ta positron spectrum, and deduced Q_{EC} = (4080 ± 100) keV for ^{176}Ta. Moreover, the latter investigators reported the total positron intensity relative to the K-conversion intensity for the 1159-keV multiplet to be $I_{\beta+}/I_{K1159}$ = 26. By combining these data with our own γ-ray and conversion-electron intensity data, we have previously calculated[8] absolute β^+ - EC intensities together with log (ft) values for decay of ^{176}Ta to levels in ^{176}Hf. Further information has been provided by Boddendijk and coworkers,[11] who have carried out two experiments which indicate a Q_{EC} value of for ^{176}Ta decay of $(3.05 \begin{smallmatrix} + 0.38 \\ - 0.04 \end{smallmatrix})$ MeV and a total positron intensity of (0.38 ± 0.04)%. The first result follows independently of any knowledge of γ-ray intensity balances and seems more reasonable than the 4.08-MeV value of Fominikh et al.,[14] in consideration of the lack of evidence for the population of levels in ^{176}Hf above 3.0 MeV. It is unlikely that a series of levels associated with the lowest observed log ft values for ^{176}Ta EC-decay would occur at 3 MeV, and that no levels at all would be populated at energies higher than this if Q_{EC} were really as high as 4 MeV.

Using only our γ-ray intensity balances for the ^{176}Hf levels, we can show that either the 3.0-MeV β^+ component reported by Fominikh et al. does not belong to ^{176}Ta, or that the relative intensity $I_{\beta+}/I_{K_{1159}}$ cannot have the value 26 as reported by those authors. We can safely ignore the small EC-β^+ feeding to the ^{176}Hf ground and first excited states, since our total γ-ray intensity imbalance for all other states is about 1900 (in the units of Table I). From simple intensity balance we know that about 12% of the EC-β^+ decays feed the 1248-keV level. Were Q_{EC} to be 4.0 MeV, one would find from theoretical

β^+/EC ratios that the feeding of this level alone would account for 1.4% β^+ intensity. Further, by summing all of our intensity imbalances, we find that Q_{EC} = 4.0 MeV implies nearly 4% β^+ feeding to levels above the ground band of ^{176}Hf, or almost twice the value 2.3% deduced by combining our (1159 + 1157 + 1155)-keV K-conversion coefficient data with the ratio $I_{\beta+}/I_{K_{1159}}$ = 26 given in Ref. 14.

We thus concur with the conclusions of Boddendijk et al., that Q_{EC} for ^{176}Ta must be appreciably less than 4.0 MeV. However, our data do not support their results for the total β^+-branching intensity. The measurement of the 511-keV annihilation γ-ray is complicated by the presence of γ-rays at 507.8 and 512.3 keV. Because of this Boddendijk et al. employed a coincidence experiment to deduce the annihilation γ-ray intensity.

We have studied this region of the γ-ray spectrum with a high-resolution (1.0 keV FWHM at 122 keV) large-volume Ge(Li) detector (35 cm^3; 24:1 ^{60}Co peak-to-Compton ratio). With use of standard peak shapes obtained experimentally, we are able to resolve the triplet of peaks at 507.8, 511.0, and 512.3 keV, and thus we can measure directly the 511-keV annihilation γ-ray intensity. Our measurements were carried out with a ^{176}Ta source placed between two 6-mm thick Al absorbers with a source-to-detector distance of about 45 cm. From our data we conclude that the total β^+-decay intensity of ^{176}Ta is (0.69 ± 0.09)% of all decays. This is higher than the value (0.38 ± 0.04)% reported by Boddendijk et al., but considerably lower than the value implied by the data of Fominikh et al.

Having established that the β^+ feeding to ground is quite small, we can deduce the absolute β^+ feeding to the 1248- and 88-keV states of ^{176}Hf by

making use of our (511 + 512)-keV coincidence data. Figure 13 shows the coincidence spectrum of interest. The decay scheme (Fig. 7) and our singles-relative-intensity data show that β^+ feeding to the 1248-keV level accounts for virtually all of the 1159-keV γ-ray intensity in the (511 + 512)-keV coincidence spectrum of Fig. 13. Similarly, the fact that essentially all of the 1357-keV intensity in Fig. 13 arises from the 512-keV coincidence provides a convenient intensity normalization; one finds after correcting for the 1155-keV γ-ray intensity that (0.10 ± 0.04)% β^+-decay to the 1248-keV level accounts for the remaining 1159-keV coincidence intensity. A similar number is obtained from the 511-keV γ-ray intensity in the 1159-keV coincidence spectrum (Fig. 4). One also finds, from theoretical EC/β^+ branching ratios[17] and from the known 12% EC-β^+ feeding of the 1248-keV level, that the experimental ratio EC/β^+ = (119 ± 50) for that level corresponds to $Q_{EC} < 3.18$ MeV. Since we observe γ-rays in the ^{176}Ta spectrum up to 2995 keV we may safely restrict the lower limit of the decay energy to 3005 keV, and we thus obtain for Q_{EC} ^{176}Ta decay the value $(3050 \,^{+\,125}_{-\,45})$ keV, in agreement with the value $(3.05 \,^{+\,0.38}_{-\,0.04})$ MeV reported by Boddendijk *et al.*

Assuming a total conversion coefficient of 6.1[10,15] for the 88-keV transition, we further conclude on the basis of the 88-keV coincidence intensity in Fig. 13 that the β^+-feeding to the 88-keV level is (0.14 ± 0.12)%. After correcting for β^+-branching to levels other than those at 88 and 1248 keV, we obtain the β^+ intensity to ground, (0.42 ± 0.17)%. These data are consistent with the factor-of-two enhanced feeding to the ground 0+ state that one expects from simple angular-momentum coupling coefficients if the parent ^{176}Ta state is ($I\pi K$ = 1-1).

The EC-β^+ feeding indicated in Fig. 7 has been derived by combining the quantities Q_{EC} = 3050 keV for ^{176}Ta and I_{β^+} = 0.69% with our γ-ray intensity balance for each level. Since the γ-rays that we are unable to place in the level scheme represent only about 7% of the total observed photon emission intensity for ^{176}Ta decay, the errors in the assigned EC-β^+ feedings arise primarily from the combined individual γ-ray intensity errors, and unless otherwise indicated may be taken to be 10-15%.

Because electron screening effects may make unreliable the use of nomograms for obtaining (ft) values of very low energy EC- and β-decays, we have used the numerical electron wave functions of Band et al.[16] to calculate log (ft) values for ^{176}Ta and ^{176m}Lu decay. The method is described in an appendix to this paper. As expected, the log (ft) values for ^{176}Ta decay obtained by this method agree very well (< 0.1 unit deviation) with the nomogram values[17] until E_{EC} becomes less than about 300 keV, where the K-shell binding energy becomes important.

The ^{176}Ta ground-state assignment of Valentin et al.[18] as 1-1(7/2 + $[404]_p$, 5/2 - $[512]_n$) has been presumed to be correct, and in some cases it is used along with log (ft) values to support spin and parity assignments (discussed in the next section). However, our experimental data indicate that the ^{176}Ta ground state may contain appreciable mixing of other components as well.

3. Spin and Parity Assignments

Although it is difficult to make assignments of spins and parities to the ^{176}Hf levels on the basis only of ^{176}Ta K-conversion electron data, log (ft) values, and γ-ray relative intensities, nevertheless we can draw some conclusions in this regard:

1149.9- and 1226.6-keV levels:

The two lowest levels above the ground rotational band (Fig. 7) are almost certainly themselves members of the same rotational band. As already indicated, the E0 transition at 1149.9-keV confirms unambiguously the assignment of an ($I\pi K = 0 + 0$) level at that energy. The level at 1226.6-keV is designated ($I\pi K = 2 + 0$) on the following basis: 1) the enhanced K-conversion coefficient associated with the 1138-keV line ($\alpha_K = 2.3 \times 10^{-2}$) indicates an E0 component; 2) the presence of the 936.4- and 1226.8-keV transitions identifies the spin as 2, and therefore the parity is necessarily even; 3) branching ratios to the ground band indicate K = 0 as the most likely assignment.

1247.7- and 1313.3-keV levels:

The level at 1248-keV can be definitely assigned as 2- on the basis of γ-ray branching and conversion coefficient data. The 1159-keV transition to the 2+ state of the ground band displays the strongest photon intensity of any line in the ^{176}Ta spectrum. Coincidence data unambiguously confirm the much weaker feeding to ground and to the 4+ ground band member. The 1247.7-keV γ-ray is essentially pure M2 from K-conversion coefficient data, while the 957-keV transition is nearly pure E3 (the M2 component may be strongly retarded by angular-momentum coupling rules if $K_i = 2$, but the data suggest there may be appreciable collective enhancement of the octupole de-excitation mode). One expects, then, that the 1159-keV transition proceeds from the 2- state and is predominantly E1. There remains, however, the question of the K-quantum-number assignment. A K = 1 assignment, though perhaps otherwise acceptable, must be discarded because of the absence of the spin-1 member of the band, a state which ought to be strongly populated by both ^{176}Ta and ^{176m}Lu decay if it exists. In

harmony with the preferred K = 2 choice is the apparent M2 admixture in the 1159-keV transition, not unexpected for a K-forbidden E1.

A definite assignment of spin 3 and odd parity can be made for the level at 1313.3 keV on the basis of conversion data, the high log (ft), and the absence of a transition to ground. Again, the K-quantum-number assignment is not unambiguous, though it is probably the same as that of the 1247.7-keV level. Our preference is to interpret these two levels as members of a K = 2- band, and there is some evidence for the intraband cascade transition from coincidence data.

1293.2-, 1341.3-, and 1379.4-keV levels:

The ($I\pi K = 0 + 0$) designation for the state at 1293.2-keV is, on the basis of the conversion data, again an obvious assignment. It is of particular interest to be able to identify the 2+ member of this second 0+ band. Though we have two candidates for such a state, we are unable to make an unambiguous ($I\pi K = 2 + 0$) assignment to either one. The first possibility is the level at 1341-keV, but it seems more likely on the basis of γ-ray branching and from the relatively "normal" 1253-keV K-conversion coefficient that this state is ($I\pi K = 2 + 2$). (K-conversion and the K/L ratio seem to indicate that the 1253-keV transition is (M1 + E2) in character.)

With the 1341-keV state thus accounted for, there is only the 1379.4-keV level. This level could be either a 2+ or 2- state. However, the conversion-electron data do not support a 2- assignment: the K-conversion coefficient of the presumed E1-(M2) 1291-keV transition appears to be far too large for even an M2 transition. Our fit (Fig. 11) to the electron complex at 1290-1293 keV indicates a K-conversion coefficient of perhaps 1.9×10^{-2} for the 1291-keV line--a number that seems to classify the transition as being (E2 + E0) in nature.

But the complication of the 1223-1225 (M+N) lines and the very strong 1293-keV E0 K-electron line in this region may have compromised the reliability of the computer fit to the 1291-keV component. The 1089-keV conversion coefficient is also uncertain, though it appears large enough to be compatible with an M2 assignment. Nor can the γ-ray branching data provide a clear choice. Although anomalous γ-ray branchings are often found, the branching to the ground rotational band is in this case so very much different from what one normally expects for a ($I\pi K = 2 + 0$) state that a 2- assignment would be favored if the electron data did not argue otherwise.

We therefore propose ($I\pi K = 2 + 0$) for the 1379.4-keV level. The weak 1379.3-keV transition has (because of its importance) in this instance been included in the level scheme, even though it is too weak to be identified in the coincidence data. If the 1379.3-keV transition is in fact correctly placed in the level scheme, then the (2 + 0) assignment would seem even more certain.

1404.6-keV:

The level at 1404.6-keV could be the 3+ member of the K = 2 band ostensibly beginning at 1341-keV, but we do not find the expected 1316-keV transition to the ground-band 2+ state. Another assignment is possible, however: because the 1404.6-keV state de-excites via the 91.2-keV transition to the 1313.4-keV level, it could be the 4- member of the K = 2 band with other members presumably at 1247.7 and 1313.3-keV. The 156.8-keV line can then be interpreted as the (4- → 2-) crossover E2 transition (an interpretation consistent with the conversion-electron data), and the 91.2- and proposed 65.7-keV (not observed in singles) lines would fit in as the cascade M1-E2's. We have adopted

the (4-2) assignment, but this assignment too presents difficulties: (1) The K-conversion of the 1115-keV transition seems too great for an E1, although there could be M2 admixture. Moreover, the 1115-keV line itself is complex, the other component being an apparent M1 de-exciting the 2949-keV state; (2) More significantly, there is an appreciable discrepancy between the measured 1115-keV energy, and that expected from energy sums. The following sums apply:

1114.96	1247.64	1313.30
+ 290.19	+ 156.84	+ 91.23
1405.15	1404.48	1404.53

This energy discrepancy could be interpreted as indicating two levels near 1405 keV. However, the coincidence data do not support such an interpretation, because both the 1115- and 156.8-keV transitions are in coincidence with the 519.7-keV transition. Ignoring the possibility that the 519.7-keV transition itself is a doublet, we dismiss the energy discrepancy as being due to the complexity of the 1115-keV region. To support further our (4-2) assignment, we note that Harmatz et al.[2] proposed an (E2 + M1) multipolarity for the 91.2-keV transition on the basis of L-subshell ratios, which is consistent with our intraband assignment for this line.

1445.8 keV:

An assignment for the 1446-keV level cannot be made with certainty, but we prefer a 3 + 2 assignment. Because of the complexity of their K-lines, the 1155- and 1358- keV transitions de-exciting this level cannot provide unequivocal conversion-coefficient information which could identify the parity. Support for the even-parity interpretation is given by the 466.2-keV M1 transition, coming from the 1912-keV (even-parity) level. Evidence against the even-parity

interpretation is that the 512-keV transition, coming from the 1958-keV (odd-parity) level, appears to have a conversion coefficient compatible with predominantly M1 character. There is some indication, however, that the 512-keV line may be complex, and at least two alternative explanations for the high 512-keV electron intensity are possible: 1) the 507.5-keV coincidence spectrum shows lines at $\approx$ 512.1 and $\approx$ 519.7-keV, and this raises the possibility of a weak 511.7-keV line de-exciting the 2944-keV level, and implies that the stronger 512-keV transition de-exciting the 1958-keV level may in fact be E1 rather than M1 in character; 2) The presence of E0 mixture in the 1223-keV transition de-exciting the 2471-keV level suggests the further possibility of E0 mixing in a weak unobserved 512.6-keV transition to yet another (2-2) state identified at 1958.1 keV. Unfortunately, the coincidence data are not sufficient to confirm either of these two possibilities, though the ambiguity could presumably be removed by a simple e^--γ coincidence experiment. Thus, the (3 + 2) assignment for the 1446-keV level remains in doubt.

For levels above 1450 keV, the a priori basis for assigning spins and parities is for the most part quite weak. However, several assignments do seem fairly certain, and some additional assignments may be deduced from a few simple model-independent assumptions. We mention below the spin-parity assignments that seem most reliable, and the basis for each one:

1643.4-, 1710.2-, 1819.0, and 1856.9-keV levels:

The level at 1643 keV is assigned ($I\pi K = 1 - 0$) on the basis of conversion coefficients and branching. The state at 1710.2-keV appears to be (3 - 0), and from the energy spacing we are inclined to consider these two states as belonging to the same rotational band. The apparent absence of the corresponding even-parity band members, at least below 1800 keV, makes it seem

likely that this band has appreciable octupole collectivity. The 0- and 2- members may then be expected to lie at somewhat higher energies. At 1819.0 and 1856.9 keV we find two levels quite selective in their decay properties. Both feed only the (1 - 0) and (3 - 0) states just discussed. The 1819-keV level de-excites via a 175-keV transition, predominantly M1, to feed the (1 - 0) state at 1643 keV. The 1857-keV level decays via 213.5- and 146.7-keV transitions, also predominantly M1 (from conversion coefficients), to feed the (1 - 0) and (3 - 0) states, with branching that is consistent with interpreting the parent state as (2 - 0). To summarize, we propose that the levels at 1643, 1710, 1819, and 1857 keV belong to the same (K = 0-) band, with the odd-parity members lowered in energy some 200 keV by the collective octupole interaction.

1672.3 and 1704.6 keV:

Information on the spin and parity of the 1672-keV level and what appears to be its rotational band member at 1704.6 keV is obtained largely from the strong 190- and 158- keV M1 branching from the 1863-keV level, which is almost certainly (1 +). The levels at 1672.3 and 1704.6 keV are on this basis assigned ($I\pi K = 1 + 1$) and (2 + 1) respectively. Moreover, branching from the 1912-keV state indicates the 3+ band member may lie at 1786.1 keV, but this assignment must be considered more tentative. Further support to this interpretation seems to be indicated by the 125- and 207-keV coincidence data, which show some evidence for the presence of the intraband cross-over and cascade transitions.

1722.1 keV:

This state is assigned spin-1, odd parity, on the basis of the 1722- and 1643-keV E1 transitions to the ground band. The K quantum-number is not obvious from γ-ray branching: since the reduced 1722- and 1643-keV intensities are

nearly equal, the branching is not in harmony with K = 0, but neither does it argue strongly for K = 1. However, it seems possible that the 2- state at 1767.5-keV belongs to such a K = 1- band (see below) and candidates for the 3- band member exist at 1793.7 and 1854.0-keV. If the rotational spacing is normal, the higher-lying state would seem the more likely 3- band member. We prefer the K = 1 assignment for the 1722-keV level for consistency with feeding from higher-lying levels, and because the K = 0 alternative is not more favorable on the basis of γ-ray and EC branching.

1767.5 keV:

The 1679.2-keV transition to the ground-band 2+ state is E1 from conversion data. In the absence of evidence for branching to the 0+ or 4+ ground-band members, the 2- assignment seems quite certain. We prefer a K = 1 assignment over K = 2 or K = 0 for reasons already given, and because of the apparent purity of the 1679-keV E1.

1862.8 and 1912.0 keV:

Conversion coefficients indicate the transitions from this level to the ground band are M1, and branching is consistent with K = 1. It seems likely from feeding to the lower-lying (K = 1+) band members at 1672 and 1705-keV that the 1863- and 1912-keV levels are both members of this second (K = 1+) band.

1924.6 keV:

The K-conversion line of the 1836-keV transition is too weak to be observed, indicating that the transition is probably E1. Although the branching to the 1248-keV 2-2 band members seems to favor a K = 1 assignment, this interpretation would make it difficult to explain the very weak feeding to ground. Therefore we prefer the alternative K = 2 assignment.

1958.1 keV:

This level is also given an ($I\pi K = 2 - 2$) assignment, and in this case the arguments are stronger than in the preceding case. The 710- and 644-keV M1 branches into the 1248-keV 2-band are quite strong, and their relative intensities argue for the (2-2) parent. The relatively low log (ft) for EC-decay to the 1958-keV level is also compatible with a spin 2- assignment. An inconsistency with regard to the 512-keV transition that de-excites this level prevents the definite characterization of the lower-lying level at 1446-keV. Conversion data indicate that the 512-keV line is M1, but this is not in harmony with the preferred 3+ assignment for the 1446-keV level. However, as pointed out earlier, there is a possibility that the 512-keV line may be complex.

2265.2-keV:

This state is characterized ($I\pi K = 2 - 2$) on the basis of the E1 multipolarity of the 924-keV γ-ray, the γ-ray branching to other levels, and the relatively low log (ft) for EC feeding.

2470.7-keV:

This state is quite remarkable because of the character of the 1223-keV transition that de-excites it to feed the 2-2 level at 1248 keV. The only reasonable explanation for the very large 1223-keV conversion coefficient is E0 competition with the γ-ray decay mode. A logical alternative interpretation of the data would be provided by postulating a third 0+ state at either 1223, 2373 or 2516 keV, but there is no additional experimental evidence to support such a postulate. The 1157.4-keV branch to the (3-2) band member is apparently pure M1. If the 1223-keV transition is, as it seems, (M1/E2 + E0), the 2471-keV

level is necessarily ($I\pi K = 2 - 2$), an assignemnt that is consistent with the remaining data. The low log(ft) for EC population of this state, and the monopole competition with M1 or E2 decay to the 1248-keV level suggest that the 2471-keV state is made up of a β-vibration superimposed on the lowest (2-2) excitation.

2912.2-, 2920.4-, 2944.1-, and 2969.0-keV levels:

EC decays to the states at 2912, 2920, 2944, and 2969 keV display log(ft) values of ≈ 4.7, ≈ 4.6, ≈ 4.3, and ≈ 4.8, respectively, suggesting that the decays are of the allowed unhindered type. Although only the state at 2920.4-keV can be immediately characterized with respect to spin, parity, and K-quantum number, the EC population ratios and the de-excitation patterns for the other three states strongly suggest the inter-relation of all four states.

In the case of the 2920.4-keV state, branching to the ground band unambiguously indicates ($I\pi K = 1 \pm 0$). The parity is almost surely negative, as indicated from the low log(ft) for EC feeding and also from the weak K-conversion associated with the 2832.0 and 2920.4-keV transitions. Though we are uncertain of the Si(Li) electron detector efficiency at 3 MeV, our estimate would have to be in error by almost an order of magnitude to place the E1 assignment in doubt.

The 2912-keV level is thought to be ($I\pi K = 0 - 0$) since it decays only to the (1-0) and (1-1) states at 1643 and 1722 keV. Within this picture, the 1-0 band member is the 2920.4-keV state, and the (2-0) member is thought to lie at 2069.0 keV. The latter state also decays predominantly to the 1643- and 1722-keV band members, although there is tenuous evidence for very weak feeding to the (2-2) 1248-keV level. Our interpretation of these three states as forming a single rotational band also seems consistent with angular momentum

coupling rules: for ℓ=1 EC-decay to a K=0 band, the geometrical (Alaga) branching relations would predict log(ft) = 4.78, 4.60, and 5.08 (normalized to 4.60) for branching to the spin-0, 1, and 2 band-members. The experimental values are 4.7, 4.6, and 4.8. Though the latter number appears somewhat small, the extreme sensitivity of the log (ft) values to the Q_{EC} assumed for such low-energy transitions places this number well within the range of expected experimental error.

There remains the 2944.1-keV state, which is populated with the lowest log (ft) in the entire ^{176}Ta decay scheme. The state decays primarily by intense M1 radiation, populating the spin-2 and 3 members of the 1248-keV 2- band. Branching is quite consistent with an ($I\pi K = 2 - 2$) assignment for the 2944-keV level. As we shall show later, it seems likely that this level and the three just discussed are all 4-quasiparticle states, the K = 0 and K = 2 projections arising from coupling of (K = 1 +), or (K = 6 +), two quasi-proton and (K = 1 -), or (K = 8 -), two quasi-neutron configurations. Such an interpretation can account quite well for the observed EC feeding and γ-ray de-excitation of these levels.

Finally, we point out that we have somewhat reluctantly assigned a separate level at 2921.0 keV. Persistent inconsistencies in the energy calibrations for the high-lying 2832.0- and 2920.4-keV doublet compared with the energy sums of intermediate-energy γ-rays de-exciting the level(s) at about 2921-keV have forced us to conclude that there are indeed two levels separated in energy by only 0.6-keV. Consideration of the feeding that would be required of the single known ($I\pi K = 1 - 0$) level at 2920.4 keV supports our conclusion. Coincidence data indicate that the 1064.0-, 1579.7-, and 1673.4-keV transitions

feed the 1856.9 ($I\pi K = 2 - 0$), 1341.3 (2+2), and 1247.7-keV levels, while the 1540.8-, and 1693.7-keV transitions feed the 1379.4 (likely 2 + 0) and 1226.6 (2+0) levels. Energy sums for the latter two transitions are consistent with the 2920.4-keV parent level, while the first three transitions all yield energy sums of (2921.0 ± 0.2) keV. However, it should be pointed out further that all of these lines are in complex regions of the spectrum, and though it seems unlikely, it is not inconceivable that the 1-0 level at 2921-keV may feed K = 2 states, and that an unfortunate +0.5-keV random error in the energy measurements of the three lines concerned may have led us to an erroneous conclusion.

From γ-ray singles data, it is evident that other states up to at least 2995.4 keV are populated by ^{176}Ta decay.

E. Decay of 3×10^{10}-Year ^{176}Lu

The 2.6%-abundant, naturally-occurring mass-176 isotope of lutetium has been studied by numerous investigators and has been found to have a β^--decay half-life of $\approx 3 \times 10^{10}$ years.[17] The β^--endpoint energy was reported by Dixon et al.[19] to be 425 ± 15-keV. We shall comment further on this datum in connection with our discussion of the ^{176m}Lu decay.

Dixon et al. also measured the γ-ray spectrum of ^{176}Lu with NaI(Tl) scintillation detectors. We here report our re-measurement of the energies of the three γ-rays arising from decay of natural ^{176}Lu. In particular, we find the energy of the γ-ray transition leading from the 6+ to the 4+ member of the ^{176}Hf ground rotational band to be 306.9 ± 0.1-keV. This datum establishes that the 6+ state lies at 597.1 keV. The other γ-ray energies (202 and 88 keV)

are well-known from ^{176}Ta decay data. No evidence is found for the presence of an 8+ → 6+ γ-ray transition in ^{176}Hf, and we conclude that there is no appreciable β-decay feeding of the spin-8 ground band member of ^{176}Hf.

F. Decay of 3.7-hour ^{176m}Lu

A 3.7-hour isomer of ^{176}Lu has been identified in previous work,[17] and it is found to β-decay essentially 100% to the ground and first excited states of ^{176}Hf (cf. Fig. 7). The isomer has recently been characterized as ($I\pi K = 1 - 0$) by Minor et al.[20]

Scintillation spectroscopy carried out by Rezanka et al.[21] appeared to indicate very weak β-feeding to a ^{176}Hf level proposed to lie at 1.14 MeV. Weak γ-rays at 1.14 and 1.05 MeV were reported in this early work, and they were assumed to populate the ground and first excited states of ^{176}Hf. It thus seemed reasonable to expect that ^{176m}Lu decay might feed one or more of the lower-lying levels deduced from the ^{176}Ta decay data. Therefore, as part of this study we have examined the γ-ray spectrum of ^{176m}Lu in the region around 1 MeV.

We prepared sources of ^{176m}Lu by irradiating 99.94% samples of $^{175}Lu_2O_3$ with thermal neutrons ($\phi = 5 \times 10^{13}$ n/cm^2/sec) for periods of time ranging from 15 to 30 minutes. Because of the rapid "growth" of the ^{177}Lu (6.8 day) activity, no chemistry was performed in order that the samples could be counted as soon as possible after the end of irradiation. A calibrated Au-Cd-Cu absorber was employed to attenuate the Hf x-rays and the very strong 88.35-keV γ-ray.

In Fig. 14 we show the γ-ray spectrum of ^{176m}Lu in the region 900 - 1330-keV, taken with a 35 cm^3 Ge(Li) detector. The spectrum clearly indicates feeding to the 1150-, 1227-, 1248-, and 1293-keV levels in ^{176}Hf

established from the ^{176}Ta decay data. Several weak unlabeled peaks are due to unidentified longer-lived ($t_{1/2}$ > 5 hours) impurities. In Table III we list the relative intensities of the γ-rays observed from the decay of ^{176m}Lu. The ^{176m}Lu data support the level scheme deduced from ^{176}Ta decay data (cf. Fig. 7) and indicate that $(1.4 \pm 0.3) \times 10^{-3}$% of the ^{176m}Lu decays feed the higher-lying ^{176}Hf levels. This number is in agreement with the value (1.3×10^{-3})% earlier reported by Rezanka et al.[21]

G. Q-values and Log(ft) values for β-decay of ^{176}Lu and ^{176m}Lu

There has been some confusion in the literature with regard to the values of Q_{β^-} for ^{176}Lu and ^{176m}Lu. Our observation of the 1204.8-keV γ-ray confirms that the 1293-keV level in ^{176}Hf is fed by ^{176m}Lu decay, but we fail to observe γ-rays that would indicate feeding to higher-lying levels. Therefore, we can establish likely limits $1300 < Q < 1375$ keV for the ^{176m}Lu decay energy on the basis of γ-ray data alone. These data are in harmony with the weighted average of several measurements of Q_{β^-} for ^{176m}Lu reported by Nuclear Data Sheets[22] to be (1318 ± 5) keV.

The recent ^{175}Lu(d,p)^{176}Lu work of Minor et al.[20] seems now to resolve as well the problem of the ^{176}Lu ground-state energy. These authors find (d,p)Q for this reaction to be (4848 ± 3) keV and observe a 1^- state at 126.5 keV, apparently confirming the location of the 3.70-hour ^{176}Lu isomer at that energy. Their data imply a correction of +170 keV to the early results of Dixon et al.[19] which indicated E_{max} = (425 ± 15) keV and Q_{β^-} = 1.02 MeV for ^{176}Lu decay. The Q-value data of Minor et al. may also be combined with the earlier ^{176}Hf(d,p)^{177}Hf results of Rickey and Sheline[23] and with the known Q-value

for ^{177}Lu β^--decay[17] to deduce independently the value, Q_{β^-} = (1195 ± 8) keV for decay of the spin-7 ground state of ^{176}Lu to ^{176}Hf. The combined ^{176m}Lu and ^{176}Lu data suggest that the correct value Q_{β^-} for ground-state ^{176}Lu decay is (1193 ± 5) keV.

Because of the very small amount of energy (25 - 165 keV) available for ^{176m}Lu decay to the ^{176}Hf levels around 1 MeV, it is not reliable to use nomograms for obtaining log(ft) values. The values indicated in Fig. 12 were calculated from the electron wave functions of Band et al.[16] according to the procedure described in the appendix to this paper.

III. DISCUSSION OF THE ^{176}Hf LEVEL SCHEME

A. Comparison of the Level Structure with Theory

Although many of the observed ^{176}Hf levels have yet to be characterized with respect to spin and parity, it seems useful to summarize briefly the assignments which have been made, and to compare them with recent theoretical calculations of the ^{176}Hf level structure. In Fig. 15 are shown the relevant experimental and theoretical data.

Most of the calculations performed to date for ^{176}Hf have been rather limited in scope or specialized in emphasis. The earliest calculations shown are those of Bes and coworkers[24,25] for the β- and γ-vibrational states. The 0 + β-vibrational excitation is predicted to lie at 1420 keV and the first 2+ (γ-vibrational) excitation is thought to lie near 1870 keV for equilibrium deformation $\delta = 0.25$. It appears quite certain that the lowest 2+ state in ^{176}Hf lies at 1341-keV, in considerable disagreement with the theories of Bes and also of Malov and Soloviev.[26] Both groups predict the first 2+ state should lie some 400-500 keV higher.

The calculations of Malov and Soloviev were carried out with single-particle energies and wave functions from a Saxon-Woods potential for A = 181. Aside from their results for the first 2+ and 1- states, agreement of their calculations with experiment is very good. Both these authors and Neergård and Vogel[27] predict the first 1-1 state to lie below the first 1-0 (octupole vibrational) excitation. Experimentally, we find that it lies about 80 keV above the 1-0 state. Of particular interest in the calculations of Neergård and Vogel are their predictions for the collective octupole enhancement of E3 matrix elements between ground and the negative-parity bands. For the transitions

de-exciting the 1248-keV level, we observe that an apparent E3 dominates what should be the preferred M2 decay mode to the 4+ ground band member. Although the Clebsch-Gordan angular momentum coupling rules favor E3 over M2 by almost an order of magnitude, the single-particle E3 lifetime estimate is about 10^{-6} sec, while the M2 estimate is only 10^{-9} sec; the M2 mode should still be favored by a factor of 100. Neergård and Vogel predict that B(E3; 0 + 0 → 3 - 2) in ^{176}Hf should be about six times the single-particle rate. We have no direct lifetime measurement for the (2-2) state, but the experimental ratio T(E3)/T(M2) for the (2-2 → 4+0) transition is > 3, which implies a substantial E3 enhancement and/or M2 hindrance for this transition.

Neergård and Vogel[27] have also considered the appreciable influence of Coriolis coupling between the negative-parity bands, and they give results for the rotational spacing in each band. However, these values are strongly dependent upon the band-head locations; therefore, we do not show in Fig. 19 their rotational band results except for the low-lying K = 2- band, which shows excellent agreement with experiment for the 2-, 3-, and 4- spacing.

Also reproduced in Fig. 15 are results of the recent investigations by Mikoshiba et al.[28] into the nature of excited 0+ states in deformed nuclei. These authors have considered in some detail the possible influence of pairing-field vibrations on the 0+ states in deformed rare-earth nuclei. In doing so, they have extended the earlier work of Bes and Broglia[29] to consider the coupling of quadrupole and pairing-field fluctuations. The properties of the ten lowest excited K = 0+ states for a number of nuclei in the rare-earth region were investigated, and the contributions of the quadrupole- and pairing-vibrations to these states were estimated.

Of particular interest here are the results of Mikoshiba et al. for ^{176}Hf, shown in Fig. 15. A decrease in the single-particle level density at 104 neutrons has been found experimentally by Burke et al.;[30] therefore, the neutron pairing-vibrational strength may be appreciable at relatively low energies in this region. Accordingly, the results of Mikoshiba et al. imply that the first and third ($I\pi K = 0 + 0$) excitations in ^{176}Hf ($\approx$ 1400 and $\approx$ 1700-keV) are predominantly of neutron pairing-vibrational character, while the second excited 0+ state ($\sim$ 1550-keV) is rather characterized by a dominant quadrupole-vibration component.

The two K = 0+ states observed in ^{176}Hf at 1150 and 1293-keV possess significantly different transition rate properties, described below, but unfortunately it is not possible to draw definite conclusions from relative intensity data as to the possible pairing-vibrational nature of these K = 0+ states. Alternative explanations which can account in a much simpler way for the widely differing properties of the low-lying ^{176}Hf 0+ excitations are also possible. Before outlining the arguments for such an interpretation, however, it seems worthwhile to summarize the derived experimental data pertaining to the low-lying K = 0+ states in ^{176}Hf.

The primary data relating to the two low-lying 0+ bands consist of γ-ray and conversion-electron intensities. Lifetime measurements are required for a detailed comparison with theory, but one useful probe of the nature of excited K = 0+ states is provided by the relative strengths of the monopole and quadrupole transitions to ground rotational band members. The usual expression is that proposed by Rasmussen[31] to compare the reduced E0 and E2 strengths:

$$X \quad \left[\frac{B(E0;\ 0'+ \rightarrow 0+)}{B(E2;\ 0'+ \rightarrow 2+)}\right] \quad = \quad \frac{\rho^2 e^2 Ro^4}{B(E2;\ 0'+ \rightarrow 2+)}$$

Similar expressions, including the proper angular momentum coupling coefficients can be written for transitions from higher-spin members of the K = 0+ bands to the ground band.

In Table IV are displayed the derived experimental data relevant to the ^{176}Hf K = 0+ excited states. It is noteworthy that the two low-lying 0+ bands exhibit values for the parameter X differing by almost a factor of 50, with the upper 0+ band exhibiting unusually high values, approaching 10. Rasmussen[31] has calculated $X = 4\beta^2$ for a uniformly charged spheroid undergoing quadrupole oscillations about an equilibrium deformation, β. An alternative formulation for the E0 matrix elements based on a microscopic model of the nuclear β-vibration was also given by Rasmussen. This treatment of the problem still predicted only $9\beta^2$ as an upper limit for X. In the extreme cases then, one might expect β-vibrations in the rare-earth region to display values $0.15 \leqslant X \leqslant 0.80$, at least an order of magnitude smaller than observed for the second ^{176}Hf 0+ excitation. Clearly, additional considerations are required to explain successfully such large values of X.

At this point it seems useful to set forth the several special features of ^{176}Ta decay that point the way to further fundamental interpretation of the ^{176}Hf level scheme. We defer to a later paper the detailed development of the interpretation, examination of alternative assignments, and the lengthy supporting arguments.

B. Summary of Theoretical Considerations

Several features of the ^{176}Hf level scheme are of particular theoretical interest. Noteworthy among these are (1) the very low log(ft) values for ^{176}Ta EC decay to some of the highest ^{176}Hf levels; (2) the abnormally high E0/E2 decay ratio from the 1293-keV 0+" state and the more normal E0/E2 ratio of the first excited 0+'; (3) the comparable beta-decay (ft) values for ground 0+ and the 0+" state, with slower decay to the 0+' state; (4) the unusually high conversion electron intensity of the 2-2 (2470.7 keV) to 2-2 (1247.7 keV) transition, signifying E0 admixture to the M1 and E2 radiative transition modes; (5) the apparent identification of the even-parity members, about 175 keV above the corresponding odd-parity members of a "collective" octupole vibrational band beginning at 1643 keV.

From the standpoint of theory ^{176}Hf lies in an interesting region where there are no low-Ω orbitals near the Fermi surface. The proton system is characterized by one pair occupying a cluster of three Nilsson levels, the nearly degenerate 7/2+ and 9/2-, with a 5/2+ just above. Likewise, one neutron pair occupies the similar cluster of 5/2-, 7/2-, and 9/2+. This dearth of low-Ω orbitals provides a condition for isomerism, and both K = 8- and K = 6+ two quasi-particle isomeric levels are known in ^{176}Hf at 1559-keV and 1333-keV respectively.[32] The available orbitals allow construction of two quasi-particle basis states of K = 1± and K = 2-, either by proton or neutron combination, and of K = 6+, 7-, and 8-, but intermediate K- values that might "short-circuit" the isomers are missing (K = 0+ bands are a special case). Likewise, four quasi-particle bands should have K-values clustering near the values 1, 7, and 14. The very high spin isomer ^{178m}Hf[33] probably derives its stability from these

circumstances, and there may well exist other such four quasi-particle isomers in Hf or W nuclei of 104 or 106 neutrons. There may also be undiscovered three quasi-particle isomers analogous to ^{177m}Lu and odd-odd isomers analogous to ^{176}Lu and ^{180}Ta.

We assume, at least as the predominant configuration, the ^{176}Ta ground-state assignment of Valentin *et al.*,[18] 1-1 [$\frac{7}{2}$ + (404) proton, $\frac{5}{2}$ - (512) neutron]. The low log(ft) transitions from ^{176}Ta to $\approx$ 3 MeV states then argue for the allowed unhindered transformation, 9/2-(514) proton → 7/2-(514) neutron. A straightforward analysis shows that such a transformation feeds only the two quasi-proton, two quasi-neutron components of K = 0- and K = 2- bands. Thus, we believe four of the highest-lying levels found in ^{176}Hf have large components of these four quasi-particle configurations. We note that they lie at energies close to the sum of the energies of the 6+ and 8- isomers constituting the main parentage of the K = 2- state.

The two low-lying 0+ excitations in ^{176}Hf are of special interest; the several works that have recently discussed theoretical interpretation of such states have been summarized by Dzhelepov and Shestopalova.[34] It seems possible, on the basis of the various microscopic models proposed, to account for both very large and very small E0/E2 branching from 0+ states. In some cases the fluctuations could apparently be ascribed to corresponding variations in the E2 moment, while in others, the E0 matrix element itself may become quite large. Experimental data for low-lying 0+ states are unfortunately quite limited, and in ^{176}Hf, which is the most unusual case yet observed in the rare-earth region, we have no direct measurement of the excited 0+ lifetimes; the unusually large E0/E2 branching from the 1293-keV state could result from retardation of the E2

transition moment, from an enhancement of the E0 strength or from a combination of both effects. Nevertheless, the β-decay feeding from both ^{176}Ta and ^{176m}Lu, and the E0/E2 branching ratios combine to yield substantial information on the nature of these two 0+ states in ^{176}Hf, and their unusual properties can apparently be explained in a rather simple way:

The 0+" state with strong E0 decay is likely the ^{176}Hf analogue to the non-collective lowest root of Soloviev's calculations[35] on ^{178}Hf, roughly half-and-half two quasi-proton excitation in each of the orbitals 7/2+ (404) and 9/2- (514). Our calculations indicate that such a state should exhibit a large E0/E2 ratio of de-excitation to the ground band. Furthermore, with such character the 0+" state should have beta decay (ft) values comparable to those of the ground state. The 0+' state is evidently more of a collective state, receiving less beta decay, and exhibiting the E0/E2 ratio of a normal beta-vibrational state.

Feature (3), the apparent E0 mixture in the 1223-keV transition from the 2471-keV state to the 1248-keV (2-2) state could well be explained by viewing the upper state as an ($I\pi K = 2 - 2$) combination of the beta vibration and the low-lying 2-2 state. This interpretation is in harmony with the E0 intensity contribution calculated for the 1223-keV K-conversion electron line, even if the photon transition is assumed to be pure E2. The alternative possibility of a similar combination with the proposed two quasi-proton 0+" state at 1293-keV seems to be ruled out by the relatively small E0/E2 branching implied by comparison of the 1223-keV conversion intensity with the 1066-keV γ-ray intensity.

Finally, the ^{176}Hf rotational spin sequence, 1-, 3-, 0-, 2- at 1643, 1705, 1819, and 1857 keV, respectively, provides what is to our knowledge the

first quantitative experimental measure of the energy splitting of odd- and even-spin members of a K = 0- band presumed to be influenced by the collective octupole interaction. Though further study is needed to confirm our interpretation of these levels as members of the same rotational band, the evidence from ^{176}Ta decay seems to support our conclusions.

It is clear that additional experimental data are necessary for a detailed interpretation of the ^{176}Hf level scheme. Of great value would be (d, t) pick-up spectroscopic studies on ^{177}Hf and (He^3, d) stripping studies on ^{175}Lu. The spectroscopic factors from such measurements could help to answer questions on the microscopic composition of the ^{176}Hf states assigned in our studies. Coulomb excitation experiments designed to determine B(E2) values to the excited K = 0+ bands would also be of interest. Verification of the tentative ($I\pi K = 2 + 0$) assignment we make for the state at 1379.4-keV could be accomplished by high-resolution study of the electron spectrum near 1290-keV, and would be most important for confirming the unusual properties of the second excited 0+ band in ^{176}Hf. Direct measurement of possible M1 - E2 mixing in the 2'+0' → 2+0 transitions would be of additional use in this regard.

APPENDIX

Log(ft) Calculations for ^{176}Ta and ^{176m}Lu Decay

The log(ft) values for both EC decay of ^{176}Ta and β-decay of ^{176m}Lu have been calculated with use of the numerical tabulation of Band et al.[16] for the bound and continuum electron wave functions at the nuclear surface.

For electron-capture decay the expression defining f is just

$$f = \frac{\pi}{2} (Q - B_{ns_{1/2}})^2 [g^2_{-1}(n) + f^2_{+1}(n)] \quad ,$$

for allowed capture from the $ns_{1/2}$ electron orbital, Q being the decay energy and B the electron binding energy. The quantities $g^2_{-1}(n)$ and $f^2_{+1}(n)$ are the Dirac radial wave functions evaluated at the nuclear radius, (cf. e.g., Ref. 16). For the EC-decay of ^{176}Ta, assuming Q_{EC} = 3.05 MeV, use of the above expression yields log(ft) values 0.1 - 0.2 units lower than those obtained from the simple

$$f_o = \frac{1}{C} (Q - B_K)^2 \quad .$$

When Q > 300-keV, the nomograms of Ref. 17 are quite adequate, since the electron binding energy correction is small.

In the case of ^{176m}Lu β^--decay, however, the small decay energy available for feeding ^{176}Hf levels above 1 MeV necessitates a more careful treatment. From Verall, Hardy, and Bell[36] we take the expression for the Fermi function in terms of large and small component Dirac electron wave functions at the nuclear surface.

$$F(Z, W) = \frac{1}{2p^2} (g^2_{-1} + f^2_{+1}) \quad ,$$

where p is the momentum ($= \sqrt{W^2 - 1}$).

Though it is not explicitly stated, these radial functions are evidently normalized to asymptotic values--as $r \to \infty$,

$$r^2(g_{-1}^2 + f_{+1}^2) \to 1 \quad .$$

Thus, these g and f functions at the nuclear radius are normalized in the same way as the tabulated a_{-1} and b_{-1} of Band, Guman, and Sogomonova.[16] Band et al. numerically calculated continuum wave functions with a finite, uniformly charged nucleus (instead of point charge) and a Fermi-Thomas-Dirac screened coulomb potential. Since we were dealing with such low beta decay energies from ^{176m}Lu, we felt it worthwhile to use the Band et al. calculations so as to treat screening as carefully as possible.

Before carrying out integrations over the electron energy to calculate ft values, we examined the energy dependence of Band's $(a_{-1}^2 + b_{-1}^2)$. We find that for electron energies at least as high as 80-keV for Z = 73 this electron probability is directly proportional to the momentum, p (or to the square root of the kinetic energy). (This result can be rationalized by considering that the outgoing probability flux in an asymptotically outgoing solution must be equal at the nuclear surface to that at large distance. The change in energy merely renormalizes the wave function at small distances.) Let us represent this dependence as follows:

$$a_{-1}^2 + b_{-1}^2 = p\, \gamma_Z \quad .$$

Thus, for low electron energies

$$F(Z, W) \approx \frac{\gamma_z}{2p} = \frac{\gamma_z}{2(W^2 - 1)^{1/2}} \quad .$$

Then for the ft value we have the integral

$$f = \int_1^{W_o} \frac{\gamma_Z}{2(W^2-1)^{1/2}} \; W(W^2-1)^{1/2} \; (W_o-W)^2 \; dW$$

$$= \frac{\gamma_Z}{2} \int_1^{W_o} W(W_o-W)^2 \; dW \quad .$$

Changing variables to the neutrino energy $\varepsilon_\nu (=W_o-W)$ we have

$$f = \frac{\gamma_Z}{2} \int_0^{W_o-1} (W_o-\varepsilon_\nu)\varepsilon_\nu^{\,2} \; d\,\varepsilon_\nu$$

$$= \frac{\gamma_Z}{2} \left[W_o \frac{(W_o-1)^3}{3} - \frac{(W_o-1)^4}{4} \right]$$

$$\approx \frac{\gamma_Z}{6} \times (\text{Beta decay energy in } mc^2)^3 \quad .$$

Table A1 gives the γ_Z values calculated from the table of Band et al. for 51-keV electrons.

Table A1

$Z_{(daughter)}$	33	41	49	57	65	73	81	84	88	95	98
γ_Z	2.21	3.28	4.71	7.01	10.4	15.5	24.0	28.3	35.4	53.0	62.6

We have used the above formula and table to calculate ft values for the low energy beta branches in ^{176m}Lu decay.

ACKNOWLEDGMENTS

The authors wish to thank Drs. J. M. Jaklevic, C. M. Lederer, and I. Rezanka for their many helpful comments and suggestions. We are particularly indebted to Dr. D. C. Camp for his cooperation and assistance in gathering the Compton-suppressed γ-ray data at the Livermore laboratory. This work was supported by the U. S. Atomic Energy Commission.

REFERENCES

1. J. O. Rasmussen and D. A. Shirley, University of California Lawrence Radiation Laboratory Report, UCRL-8618 (1959) unpublished.
2. B. Harmatz, T. H. Handley, and J. W. Mihelich, Phys. Rev. 119, 1345 (1960).
3. H. Verheul, H. M. W. Booy, J. G. R. Okel, and J. Blok, Nucl. Phys. 42, 551 (1963).
4. A. Hashizume and Y. Tendow, J. Phys. Soc. Japan 18, 1107 (1963).
5. F. F. Felber Jr., University of California Lawrence Radiation Laboratory Report (Thesis), UCRL-3618 (1957) unpublished.
6. D. C. Camp, University of California Lawrence Radiation Laboratory Report, UCRL-50156 (1967) unpublished.
7. L. B. Robinson, F. Gin, and H. Cingolani, Nucl. Instr. Methods 75, 121 (1969); L. B. Robinson and J. D. Meng, University of California Lawrence Radiation Laboratory Report, UCRL-17220 (1967) unpublished.
8. F. M. Bernthal, University of California Lawrence Radiation Laboratory Report (Ph.D. Thesis), UCRL-18651 (1969).
9. R. Gunnink, R. A. Meyer, J. B. Niday, and R. P. Anderson, Nucl. Instr. Methods 65, 26 (1968).
10. R. S. Hager and E. C. Seltzer, "Internal Conversion Tables," CALT-63-60 (1967).
11. H. G. Boddendijk, S. Idzenga, G. Kleimeer, and H. Verheul, Nucl. Phys. A134, 442 (1969).
12. M. J. Martin, Nuclear Data Sheets (A=176), NDS 6-6-35 (1965).
13. G. T. Garvey, W. J. Gerace, R. L. Jaffe, I. Talmi, and I. Kelson, Rev. Mod. Phys. 41, S1 (1969).

14. W. I. Fominikh, J. Molnar, N. Nenoff, B. Styczen, and J. Zvolsky, Contributions to the International Symposium on Nuclear Structure, Dubna (1968) p. 46.

15. O. Dragoun, H. C. Pauli, and F. Schmutzler, Max Planck Institute Report MPIH-1968-V14 (1968); O. Dragoun, Z. Plajner, and F. Schmutzler, MPIH-1969-V5 (1969).

16. I. M. Band, V. N. Guman, and G. A. Sogomonova, "Tables of Radial Functions and Phases of Electrons," Academy of Sciences, USSR, Leningrad (1959).

17. C. M. Lederer, J. M. Hollander, and I. Perlman, "Table of Isotopes," (1967).

18. J. Valentin and A. Santoni, Nucl. Phys. 47, 303 (1967).

19. D. Dixon, A. McNair, and S. C. Curran, Phil. Mag. 45, 683 (1954).

20. M. M. Minor, R. K. Sheline, E. B. Shera, and E. T. Jurney, to be published (1969). We thank the authors for providing us with their data prior to publication.

21. I. Rezanka, J. Frana, A. Mastalka, and J. Benes, Czechoslov. J. Phys. 12, 530 (1962).

22. M. J. Martin, op. cit., p. 1988.

23. F. A. Rickey and R. K. Sheline, Phys. Rev. 170, 1157 (1968).

24. D. R. Bes, Nucl. Phys. 49, 544 (1963).

25. D. R. Bes, P. Federman, E. Magueda, and A. Zuker, Nucl. Phys. 65, 1 (1965).

26. L. A. Malov, V. G. Soloviev, and U. M. Fainer, Contributions to the International Symposium on Nuclear Structure, Dubna (1968) p. 78.

27. K. Neergård and P. Vogel, Nucl. Phys. A145, 33 (1970).

28. O. Mikoshiba, R. K. Sheline, and T. Udagawa, Nucl. Phys. A101, 202 (1967).

29. D. R. Bes and R. A. Broglia, Nucl. Phys. 80, 289 (1966).

30. D. G. Burke, et al., cited in Ref. 29.

31. J. O. Rasmussen, Nucl. Phys. 19, 85 (1960).

32. J. Borggreen, et al., Nucl. Phys. A96, 561 (1967).

33. R. G. Helmer and C. W. Reich, Nucl. Phys. A114, 649 (1968).

34. B. S. Dzhelepov and S. A. Shestopalova, "Nuclear Structure," Proceedings of the 1968 Dubna Symposium, p. 39.

35. V. G. Soloviev, Atomic Energy Review 3, 117 (1965).

36. R. I. Verrall, J. C. Hardy, and R. E. Bell, Nucl Instr. Methods 42, 258 (1966).

TABLE CAPTIONS

Table Ia. The γ-ray transitions observed from decay of ^{176}Ta with intensity ⩾ 1% of the 710.5-keV γ-ray intensity.

Table Ib. The γ-rays observed from ^{176}Ta decay with intensity 0.20-0.99% of the 710.5-keV intensity.

Table II. Conversion-electron lines observed from decay of ^{176}Ta.

Table III. Relative intensity of γ-rays from decay of ^{176m}Lu to levels in ^{176}Hf.

Table IV. Derived values of the E0-E2 branching parameter, $X = \frac{\rho^2 R_o^4 e^2 (I_n' 200 | I_1' 0)}{B(E2)}$, for decay of K=0+ states in ^{176}Hf.

Table Ia. γ-ray transitions observed in the decay of ^{176}Ta with intensity ≥ 1% of the 710.5-keV γ-ray intensity.

E_γ(keV)[a,d]	I_γ[b]	α_K[c]	$\frac{\alpha_K}{\alpha_{\Sigma L}}$	Multipole	Level placement[e]
88.35 (4)	220.	> 8. (-1)	> 0.2	E2	88.35
91.23 (4)	1.1	> 1.1†	> 0.36†		1404.5
*125. (4)[f]	≤ 4.				1912.0
146.74 (5)	3.9	8.8(-1)†		M1(+E2?)	1856.9
156.84 (7)	6.6	3.7(-1)†		E2	1404.5
158.19 (7)	4.2	8.6(-1)†		M1	1862.8
175.50 (7)	7.8	5.1(-1)†	5.6	M1(+E2?)	1819.0
190.36 (7)	7.6	4.3(-1)	7.2	M1+E2	1862.8
201.84 (6)	105.	1.65(-1)[g]	2.0	E2	290.2
*207. (5)[h]	≤ 1.5				1912.0
213.50 (6)	9.8	2.9(-1)		M1(+E2?)	1856.9
216.00 (7)	2.2				1793.7
236.19 (7)	1.5	2.2(-1)		M1(+E2)	1958.1
239.62 (6)	10.0	2.5(-1)	≥ 5.7	M1	1912.0
264.13 (6)	1.4				1577.6
315.50 (15)	1.5(2)				[2265.2]
346.90 (20)	2.1				1924.6
350.18 (20)	1.5	8.9(-2)		M1(+E2)	2308.3
358.72 (20)	1.8				2308.3
380.48 (20)	2.4	1.8(-2)		E1(+M2)	1958.1
414.34 (15)	1.4	6.2(-2)		M1	[1793.6],[1819.0]
426.34 (15)	1.2(2)	4.7(-2)		M1+E2	[1767.5]

(continued)

Table Ia. Continued

E_γ(keV)[a,d]	I_γ[b]	α_K[c]	$\frac{\alpha_K}{\alpha_{\Sigma L}}$	Multi-pole	Level[e] placement
445.52 (8)	1.0				[2308.3],[1672.3]
461.41 (8)	1.1(2)				[(2944.1)]
466.16 (7)	20.6	4.7(-2)		M1	1912.0
473.21 (7)	5.1				2944.1
474.64 (8)	1.6				[(2066.2)],[1854.0]
507.79 (15)	26.7	3.8(-2)	6.4	M1	2432.4
512.3 (2)	7.4(7)	4.0(-2)	7.0	(M1)	1958.1,2944.1?
*519.7 (2)	(6.)				1924.6
*521.3 (1)	(5.)	≈ 3.6(-2)	≈ 8		2470.7
*521.6 (1)	(45.)				1862.8
524.90 (11)	1.1(25)				
532.54 (11)	4.5(7)	≈ 3.3(-2)			1912.0
533.23 (16)	1.2(4)				[(2482.9)]
540.27 (13)	1.1(2)				2307.8
541.24 (12)	1.7(2)				
543.18 (11)	1.5				2265.2
545.74 (11)	4.1(7)				
546.53 (10)	9.8	≈ 4.5(-2)			2470.7
569.77 (11)	2.1(3)				1862.8
570.76 (10)	8.5	3.5(-2)			1912.0,[(2482.9)]
571.30 (9)	4.9				[1819.0]
579.08 (15)	1.1				1958.1

(continued)

Table Ia. Continued

E_γ(keV)[a,d]	I_γ[b]	α_K[c]	$\frac{\alpha_K}{\alpha_{\Sigma L}}$	Multi-pole	Level[e] placement
586.72 (9)	1.6				
609.25 (9)	1.4(2)				[1856.9]
611.16 (8)	23.4	2.6(-2)	6.8	M1	1924.6
615.22 (9)	1.9(3)				[1862.8]
616.79 (8)	18.6	4.4(-3)		E1	1958.1
632.12 (9)	1.3				
638.83 (8)	3.7	$\approx$2.2(-2)			2432.4
642.85 (8)	1.8	$\leqslant$4.3(-2)			
644.86 (8)	18.4	2.1(-2)		M1	1958.1
660.67 (8)	2.2				[2969.0]
664.07 (10)	1.6(2)				[(2482.9)]
665.01 (12)	1.1(3)				[2308.3]
*677.09 (8)	5.9	$\approx$2.1(-2)			1924.6,2470.7
678.85 (8)	3.8	1.9(-2)		M1	2944.1
685.55 (8)	2.2	1.5(-2)		M1+E2	
701.96 (9)	1.3				[1949.7]
710.50 (8)	100.	1.8(-2)	6.0	M1	1958.1
717.45 (8)	1.2				
723.10 (8)	2.4	2.1(-2)		M1	[1949.7]
740.97 (9)	2.5	$\approx$3.1(-2)			
819.49 (10)	4.8	< 5 (-3)			2265.2
833.50 (10)	1.4(2)				[2791.5],[2878.2]

(continued)

Table Ia. Continued

E_γ(keV)[a,d]	I_γ[b]	α_K[c]	$\frac{\alpha_K}{\alpha_{\Sigma L}}$	Multi-pole	Level[e] placement
839.25 (11)	1.3(2)				[2905.6]
857.66 (10)	2.6				
863.19 (10)	2.2				
923.94 (8)	13.5	≈ 1.3(-3)		E1	2265.2
936.42 (8)	10.4	5.0(-3)		E2	1226.6
951.86 (10)	1.3(2)				2265.2
957.40 (8)	10.6	9.2(-3)		E3(+M2)	1247.7
960.77 (12)	1.4(2)				2817.6
962.74 (14)	1.0(2)				[2912.2],[2921.0]
967.06 (9)	2.4(3)				[2308.3]
979.94 (22)	1.1				
994.46 (12)	1.0(2)				[2307.8],[2944.1]
998.30 (10)	1.8(3)				
1002.62 (11)	1.3(2)				
1017.58 (11)	2.2(3)				[2265.2]
1023.10 (10)	49.4	1.6(-3)		E1	1313.3
1043.29 (11)	1.1(2)				
1051.03 (11)	2.0(3)				1341.3
1061.61 (9)	10.0	5.4(-3)		E2	1149.9
1064.03 (12)	1.6(2)	⩽ 1.5(-2)			2921.0
1066.20 (9)	11.9	3.7(-3)			2470.7
1089.06 (10)	3.7				1379.3

(continued)

Table Ia. Continued

E_γ(keV)[a,d]	I_γ[b]	α_K[c]	$\frac{\alpha_K}{\alpha_{\Sigma L}}$	Multi-pole	Level placement[e]
1090.94 (13)	1.4(2)				[2432.4]
1097.24 (10)	1.2(2)				
1107.81 (9)	4.7	6.1(-3)		M1	
*1115.0 (9)	9.2	6.3(-3)			1404.5,2969.0
1122.80 (9)	1.9(3)				[1413.0]
1125.45 (9)	2.6				
1138.26 (8)	12.6	2.8(-2)	≈ 4	E0+E2	1226.6
1155.5 (2)	12.0(1.5)	≈ 3 (-3)		(E2+M1)	1445.8
1157.41 (10)	62.9	5.6(-3)	≈ 4.2	M1	2470.7
1159.30 (10)	458.	2.9(-3)	6.2	E1+M2	1247.7
1174.17 (10)	3.8				2817.6
1184.55 (13)	2.0(3)	⩽ 1.4(-2)			[2432.4]
1190.22 (10)	84.1	5.4(-3)	6.6	M1	2912.2
1198.15 (11)	1.2(2)				[2920.4]
1201.48 (10)	6.7	⩽ 7.3(-3)			2969.0
1204.85 (10)	6.1	⩽ 4.7(-3)			1293.2
1211.30 (13)	1.5(2)				
1213.20 (11)	2.7				[2885.5]
1222.95 (10)	37.0	≈ 3.6(-2)	⩾ 6	E2+M1+E0	2470.7
1224.96 (10)	105.	≈ 9 (-4)		E1	1313.3
1226.85 (25)	6.8(9)				1226.6
1234.26 (15)	1.2(2)				

(continued)

Table Ia. Continued

E_γ(keV)[a,d]	I_γ[b]	α_K[c]	$\frac{\alpha_K}{\alpha_{\Sigma L}}$	Multi-pole	Level[e] placement
1239.86 (12)	2.1(3)				[2817.6],[2912.2]
1247.68 (15)	8.5(9)	1.1(-2)	≈ 5	M2	1247.7
1250.01 (18)	2.3(3)				
1252.90 (10)	57.1	3.4(-3)	7.6	M1+E2	1341.3
1258.75 (11)	3.5(5)	⩽ 6.2(-3)			2969.0
1268.78 (10)	24.6	2.5(-3)		E2+M1	2912.2
1277.90 (11)	2.9				
1287.40 (12)	1.7				1577.6
1291.01 (10)	24.6	≈ 1.9(-2)	≈ 6	(E2+E0)	1379.3
1301.10 (11)	1.4				[1591.3]
1308.30 (12)	1.2				
1325.67 (13)	1.5(2)				[2969.0]
1341.33 (10)	61.9	2.6(-3)	6.3	E2(+M1?)	1341.3
1346.08 (25)	1.3(3)				2791.5
1357.52 (10)	37.0	≈ 3 (-3)			1445.8
1366.49 (11)	4.0				2944.1
1371.75 (12)	2.8				2817.6
1379.29 (15)	1.0(3)				[1379.4]
1412.84 (11)	2.1				[2817.6],[(1413.0)]
1420.04 (10)	8.4				1710.2
1427.64 (11)	2.2				
1432.56 (11)	1.6				2878.2
1450.40 (10)	6.7				2791.5

(continued)

Table Ia. Continued

E_γ(keV)[a,d]	I_γ[b]	α_K[c]	$\frac{\alpha_K}{\alpha_{\Sigma L}}$	Multi-pole	Level[e] placement
1476.18 (10)	8.8	1.6(-3)		E2	2817.6
1489.33 (10)	13.5	1.7(-3)			1577.6
1495.85 (15)	3.5				1786.1
*1503. (7)	⩽ 2.				1793.7
1504.24 (10)	14. (2)				2817.6
1515.56 (13)	1.0				[2920.4]
1536.62 (11)	7.1				2878.2
1540.82 (11)	6.5				2920.4
1543.73 (15)	4.7				2791.5
1555.05 (10)	74.1	7.8(-4)	⩾ 3.6	E1	1643.4
1563.53 (13)	3.6(6)				1854.0
1564.95 (11)	7.6				2878.2
1579.9 (2)	5.2(5)	1.8(-3)		M1+E2	2921.0
1584.02 (10)	97.6	1.7(-3)		M1+E2	1672.3
1603.46 (18)	1.0(3)				
1608.68 (11)	2.7				
1612.63 (12)	3.2				2762.6
1616.18 (10)	23.8	2.4(-3)			1704.6
*1621.87 (10)	10.7				1710.2,1912.0
1628.53 (30)	2.5(6)				
1630.83 (10)	32.8	2.2(-3)		M1	2944.1
1633.74 (10)	54.3	6.0(-4)		E1	1722.0

(continued)

Table Ia. Continued

E_γ(keV)[a,d]	I_γ[b]	α_K[c]	$\frac{\alpha_K}{\alpha_{\Sigma L}}$	Multipole	Level[e] placement
1637.60 (18)	1.5(3)				[2885.5]
1643.45 (10)	44.4	6.5(-4)		E1	1643.4
1659.21 (11)	2.0				
1672.32 (12)	22.0	2.4(-3)	≈ 8		1672.3
1673.40 (16)	8.3(2.0)				2921.0
1679.18 (11)	22.3	5.7(-4)		E1	1767.5
1693.7 (2)	9.6	≈ 2.3(-3)	8.3		2920.4
1696.55 (13)	85.8	2.2(-3)		M1	2944.1
1697.8 (2)	6. (2)				1786.1
1704.70 (12)	25.9	1.4(-3)	⩾ 3.4		1704.6
*(1705.4)	⩽ 3				1793.7
1718.1 (4)	1.8(6)				
*1721.3	weak				2969.0
1722.04 (13)	60.6	6.0(-4)		E1	1722.0
1725.9 (4)	1.2(4)				
1745.29 (14)	2.1				
1754.94 (16)	1.3				
1765.75 (15)	8.8	1.2(-3)			1854.0
1768.22 (16)	3.4				
1774.56 (15)	28.9	1.9(-3)	10	M1	1862.8
1793.17 (15)	3.7				
1820.0 (3)	1.6(3)				

(continued)

Table Ia. Continued

E_γ(keV)[a,d]	I_γ[b]	α_K[c]	$\frac{\alpha_K}{\alpha_{\Sigma L}}$	Multipole	Level[e] placement
1823.70 (15)	83.4	1.6(-3)		M1	1912.0
1836.34 (16)	4.0	⩽ 1.0(-3)		(E1)	1924.6
1855.69 (16)	2.2				
1861.15 (25)	4.8(1.2)				1949.7
1862.74 (15)	74.0	1.6(-3)	7.6	M1	1862.8
1869.78 (16)	1.5				1958.1
1948.40 (18)	2.2(5)				
1949.80 (17)	2.4(5)	1.5(-3)			1949.7
1956.48 (15)	15.9	1.1(-3)			2044.8
1960.60 (16)	1.1				
1977.85 (15)	16.2	9.8(-4)			2066.2
2044.87 (15)	25.0	9.4(-4)			2044.8
2066.28 (16)	1.3				2066.2
2192.33 (20)	4.2	4.3(-4)			2280.7
2219.49 (20)	5.4	5.7(-4)			2307.8
2246.92 (20)	2.4				
2280.6 (2)	3.3				2280.7
2307.7 (2)	3.7	7.7(-4)			2307.8
2317.0 (2)	4.6	4.3(-4)			2405.4
2361.5 (2)	3.8				
2394.6 (2)	2.3				[2482.9]
2405.2 (2)	9.1	4.6(-4)			2405.4

(continued)

Table Ia. Continued

E_γ(keV)[a,d]	I_γ[b]	α_K[c]	$\frac{\alpha_K}{\alpha_{\Sigma L}}$	Multipole	Level placement[e]
2482.8 (2)	1.6				[2482.9]
2513.82 (20)	12.4				2602.2
2602.15 (20)	6.5(7)				2602.2
2674.2 (2)	3.4				[2762.6]
2703.4 (3)	1.3(3)				
2773.8 (2)	2.1(3)				
2789.98 (20)	1.5				--
2797.14 (20)	1.2				[2885.5]
2823.60 (40)	1.0(2)				[2912.2]
2832.00 (20)	80.5	8.8(-5)	$\geqslant 6$	E1	2920.4
2863.88 (20)	2.0				
2885.55 (22)	2.0				[2885.5]
2920.41 (20)	40.6	7.1(-5)		E1	2920.4

[a]The energy errors indicated reflect the combined statistical uncertainty associated with the peak centroid, and the systematic errors expected from system nonlinearity and from uncertainties in the standard calibration energies.

[b]Except where otherwise indicated, the error in the relative intensities is about 8%, an error arising largely from the uncertainty of the detector efficiency. Where the indicated errors exceed this figure, they reflect the statistical uncertainty, σ, associated with the computer least squares fit to the photopeak.

(continued)

Table Ia. Continued

[c]Conversion coefficients marked with a dagger (†) have been computed from the data of Harmatz et al. (Ref. 81).

[d]The starred (*) lines are complex groups we have been unable to resolve.

[e]Level assignments are indicated by three notations, depending on the basis (and relative confidence) of the assignment:

1247.7 → consistent coincidence and singles data. Placement in the level scheme will be found in Fig. 34.

[2265.2] → assigned on the basis of energy difference only. Placement is in Fig. 35.

[(2482.9)] → assigned by energy difference, and feeding or de-exciting a probable level indicated in Fig. 35.

[f]Obscured by the ^{175}Ta lines at 125.9 and 126.6 keV. We assign a ^{176}Ta line on the basis of coincidence data.

[g]Theoretical value. Assumed pure E2 for normalization.

[h]Obscured by the ^{175}Ta line at 207.4 and the ^{177}Ta line at 208.4 keV. Assignment of the ^{176}Ta line is made on the basis of coincidence data.

Table Ib. The γ-rays observed from ^{176}Ta decay with intensity 0.20-0.99% of the 710.5-keV intensity

E_γ(keV)	I_γ	Level Placement
110.1 (2)	0.36 (5)	
111.3 (2)	0.31 (5)	
117.5 (2)	0.23 (5)	
118.93 (2)	0.22 (4)	[(1710.2)]
131.0 (15)	0.40 (10)	[1924.6],[1949.7]
140.9 (10)	0.97 (10)	
173.00 (7)	0.28 (4)	[1577.6]
179.10 (6)	0.72 (7)	
185.72 (6)	0.50 (6)	
192.80 (8)	0.24 (4)	[1445.8]
196.82 (14)	0.46 (12)	[2602.2]
198.07 (12)	0.70 (15)	
230.88 (8)	0.49 (4)	
248.29 (8)	0.52 (5)	
271.58 (9)	0.24 (4)	
277.74 (8)	0.20 (4)	
280.77 (7)	0.22 (4)	
292.88 (10)	0.73 (7)	1672.3
303.55 (15)	0.42 (4)	[2905.6]
306.79 (20)	0.50 (5)	
314.53 (20)	0.57 (7)	
318.83 (30)	0.21 (4)	[2921.0]

(continued)

Table Ib. Continued

E_γ(keV)	I_γ	Level Placement
327.05 (30)	0.26 (4)	
337.51 (20)	0.23 (3)	
343.38 (20)	0.69 (7)	
361.76 (20)	0.62 (9)	[2066.2]
362.71 (30)	0.38 (9)	[1767.5]
366.20 (25)	0.24 (3)	
382.71 (25)	0.44 (8)	
383.60 (20)	0.97 (10)	[2308.3]
386.10 (20)	0.45 (5)	[2791.5]
388.06 (20)	0.56 (5)	[1767.5]
401.44 (20)	0.36 (4)	[2044.8]
411.67 (20)	0.34 (5)	
421.08 (30)	0.33 (7)	
423.15 (30)	0.32 (8)	
424.48 (15)	0.92 (10)	[1672.3]
428.85 (20)	0.27 (4)	[1722.0]
433.51 (9)	0.80 (9)	
434.85 (10)	0.89 (9)	[2905.6]
440.01 (8)	0.41 (5)	
450.94 (13)	0.31 (5)	[2307.8]
452.18 (10)	0.45 (6)	[1793.6],[1856.9]
454.63 (9)	0.32 (5)	[2762.6]

(continued)

Table Ib. Continued

E_γ(keV)	I_γ	Level Placement
459.10 (9)	0.60 (7)	[2265.2]
479.14 (10)	0.55 (7)	
480.83 (9)	0.54 (7)	[2405.4]
483.28 (9)	0.50 (6)	1862.8
494.98 (13)	0.26 (4)	
517.4 (4)	0.60 (30)	
529.08 (17)	0.26 (10)	
550.4 (5)	0.81 (20)	
551.4 (2)	0.35 (6)	[2405.4]
553.5 (2)	0.40 (6)	[1958.1]
555.2 (2)	0.27 (5)	[2265.2]
560.0 (2)	0.51 (7)	
561.6 (3)	0.25 (6)	
566.6 (2)	0.23 (4)	
577.3 (1)	0.83 (9)	[(2885.5)]
583.5 (2)	0.24 (4)	[1924.6]
584.9 (2)	0.36 (5)	
589.9 (1)	0.30 (4)	
594.9 (2)	0.23 (4)	
598.6 (2)	0.46 (8)	[1912.0]
604.6 (1)	0.48 (6)	[2885.5],[2912.2]
626.1 (2)	0.31 (5)	[(2482.9)]

(continued)

Table Ib. Continued

E_γ(keV)	I_γ	Level Placement
636.6 (1)	0.95 (10)	[1949.7],[2944.1]
656.8 (1)	0.64 (7)	
670.2 (2)	0.22 (5)	
693.2 (1)	0.38 (5)	
730.7 (1)	0.60 (7)	[2308.3]
735.9 (2)	0.30 (6)	
760.4 (2)	0.31 (5)	[2470.7]
766.5 (1)	0.56 (7)	
774.0 (3)	0.24 (6)	
779.3 (1)	0.54 (6)	
782.7 (1)	0.62 (7)	
784.2 (2)	0.34 (7)	
787.1 (1)	0.53 (6)	
789.4 (2)	0.26 (4)	
798.5 (2)	0.87 (15)	[2470.7]
799.5 (3)	0.39 (20)	
801.7 (2)	0.26 (5)	(1823.7 d.e.?)
803.8 (1)	0.65 (7)	
808.6 (1)	0.68 (8)	
837.7 (3)	0.35 (10)	
841.5 (2)	0.78 (18)	[2791.5]
842.6 (5)	0.38 (20)	

(continued)

Table Ib. Continued

E_γ(keV)	I_γ	Level Placement
861.0 (1)	0.75 (9)	[2265.2],[2905.6],[(2452.3)]
867.4 (1)	0.63 (8)	[2912.2]
872.3 (2)	0.31 (5)	
876.6 (2)	0.46 (6)	
878.4 (2)	0.45 (6)	
884.7 (3)	0.26 (10)	
886.3 (2)	0.72 (9)	
893.3 (2)	0.48 (12)	[2470.7]
900.3 (1)	0.69 (8)	
907.3 (1)	0.89 (10)	
971.8 (1)	0.89 (10)	
975.1 (2)	0.81 (10)	
977.0 (2)	0.91 (11)	
981.0 (3)	0.92 (35)	[2905.6]
986.7 (2)	0.60 (12)	
1011.1 (3)	0.57 (20)	[2969.0]
1021.0 (5)	0.66 (30)	[2878.2]
1035.0 (2)	0.46 (9)	
1052.7 (2)	0.80 (12)	[2432.4]
1112.9 (2)	0.94 (10)	[2817.6]
1148.3 (2)	0.85 (15)	[2791.5]
1178.5 (2)	0.70 (12)	[2405.4]

(continued)

Table Ib. Continued

E_γ(keV)	I_γ	Level Placement
1281.2 (2)	0.87 (13)	
1333.1 (2)	0.69 (18)	[(2482.9)]
1438.1 (3)	0.55 (12)	[2817.6]
1462.6 (2)	0.49 (10)	
1467.5 (2)	0.80 (9)	
1470.0 (2)	0.93 (20)	
1482.8 (3)	0.54 (14)	
1573.3 (2)	0.66 (16)	
1665.0 (2)	0.91 (14)	
1712.0 (3)	0.82 (20)	
1736.7 (2)	0.71 (8)	
1751.1 (3)	0.51 (9)	
1875.1 (3)	0.47 (9)	
1911.6 (3)	0.24 (5)	[1912.0]
1937.9 (2)	0.45 (7)	
1970.6 (2)	0.57 (7)	
2042.7 (5)	0.65 (22)	
2049.2 (4)	0.52 (11)	
2057.4 (3)	0.32 (5)	
2071.0 (2)	0.31 (5)	
2077.0 (2)	0.76 (9)	
2090.6 (3)	0.26 (5)	

(continued)

Table Ib. Continued

E_γ(keV)	I_γ	Level Placement
2140.1 (2)	0.72 (8)	
2162.1 (2)	0.72 (8)	[2432.2]
2257.9 (4)	0.44 (12)	
2260.4 (3)	0.57 (10)	
2272.1 (3)	0.32 (5)	
2278.6 (3)	0.49 (7)	
2304.5 (4)	0.50 (22)	
2314.8 (5)	0.50 (25)	
2374.2 (3)	0.35 (7)	
2421.7 (3)	0.37 (6)	
2460.3 (3)	0.54 (7)	
2480.5 (4)	0.80 (10)	
2506.2 (3)	0.51 (9)	
2531.6 (5)	0.40 (12)	
2534.2 (3)	0.65 (12)	
2548.4 (3)	0.63 (10)	
2571.6 (2)	0.85 (9)	
2586.1 (3)	0.63 (10)	
2681.6 (3)	0.60 (15)	
2689.7 (3)	0.85 (20)	
2705.6 (3)	0.45 (17)	
2729.3 (2)	0.65 (10)	

(continued)

Table Ib. Continued

E_γ(keV)	I_γ	Level Placement
2744.5 (3)	0.48 (7)	
2755.3 (3)	0.25 (7)	
2762.8 (2)	0.90 (12)	[2762.6]
2769.1 (3)	0.85 (9)	
2817.0 (4)	0.85 (12)	[2905.6]
2845.1 (3)	0.12 (3)	
2854.1 (9)	0.10 (7)	
2856.1 (5)	0.22 (9)	[2944.1]
2882.5 (4)	0.57 (11)	
2890.3 (4)	0.15 (5)	
2905.7 (4)	0.40 (6)	[2905.6]
2912.3 (6)	0.39 (6)	[2912.2]
2940.7 (3)	0.34 (4)	
2952.4 (2)	0.69 (8)	
2971.6 (3)	0.21 (3)	
2978.7 (3)	0.34 (3)	
2995.4 (3)	0.092 (14)	

NOTE: The convention followed for noting level assignments is the same as in Table Ia.

Table II. Conversion electron lines observed from decay of ^{176}Ta.

Transition Energy (keV)	Conversion Electron Intensity[a,b]		
	K_e-	$\sum L_e$-	$\sum (M+N)_e$-
88.4	$> 1.0 \times 10^4$	$\approx 4.8 \times 10^4$	$\approx 1.4 \times 10^4$
91.2	$> 66^\dagger$	$180^\dagger$	
131.1	$40^\dagger$		
146.7	$190^\dagger$		
156.8	$135^\dagger$		
158.2	$200^\dagger$		
175.5	$220^\dagger$	39.	
190.4	180	25.	
201.8	960	471.	
213.5	156		
236.2	18.5		
239.6	138	$\leqslant 24.$	
288.8	7.4		
314.5 + 315.4	4.5		
346.9	$\leqslant 7.2$		
350.2	7.4		
361.8	3.7		
366.2	5.5		
380.5	2.4		
382.7 + 383.6	5.7		
393.2	4.9		

(continued)

Table II. Continued

Transition Energy (keV)	Conversion Electron Intensity[a,b]		
	K_e-	$\sum L_e$-	$\sum (M+N)_e$-
414.3	4.8		
466.2	53.8		
473.2 + 474.6	≈13.		
507.8	55.9	8.7	
512.3	16.2	2.3 (5)	
519.7	⩽20.		
521 (complex)	89.4	⩽10.9	
532.5 + 533.2	≈10.		
546.5	≈24.		
571 (complex)	26.0		
611.2	33.8	⩽ 5.0	
616.8	4.5		
638.8	≈ 4.6		
642.9	4.3		
644.8	21.3		
677.1	≈ 6.8		
678.9	4.1		
685.6	3.4		
710.5	100.	16.6	3.2 + 1.3
723.1	2.9		
741.0	≈ 4.3		

(continued)

Table II. Continued

Transition Energy (keV)	Conversion Electron Intensity[a,b]		
	K_{e^-}	$\sum L_{e^-}$	$\sum (M+N)_{e^-}$
923.9	1.0 (5)		
936.4	2.9		
957.4	5.4		
1023.1	4.5		
1061.6	3.0 (5)		
1064.0	$\leqslant$ 1.5		
1066.2	2.4 (5)		
1089.1 + 1090.9	$\approx$ 2.		
1107.8	1.6 (3)		
1115.0	3.2		
1138.3	19.6	$\leqslant$ 6.	
1149.8	5.0		
1155.5	2.0 (4)		
1157.4	19.6	4.7 (1.5)	
1159.3	72.8	11.8	
1184.6	1.5 (3)		
1190.2	25.0	3.8	
1201.5	$\leqslant$ 2.7		
1204.8	$\leqslant$ 1.6 (5)		
1223.0	$\approx$ 74	11.3	
1225.0	$\approx$ 5		

(continued)

Table II. Continued

Transition Energy (keV)	Conversion Electron Intensity[a,b]		
	K_{e^-}	$\sum L_{e^-}$	$\sum (M+N)_{e^-}$
1247.7	⩽ 5.0	1.0	
1252.9	10.7	1.4	
1258.8	⩽ 1.2		
1268.8	6.1		
1291.0	≈ 25	≈ 4	
1293.2	87.3	13.9	
1341.3	8.8	1.4	
1357.5	≈ 6.4		
1476.2	0.8		
1489.3	1.3		
1504.2	2.4	0.8	
1555.0	3.2	⩽ 0.9	
1563.5 + 1565.0	1.2		
1579.7	0.5		
1584.0	9.4		
1616.2	3.1		
1630.8	4.0		
1633.7	1.8		
1643.5	1.6		
1672.3 + 1673.4	4.1	0.5 (2)	
1679.2	0.71 (13)		

(continued)

Table II. Continued

Transition Energy (keV)	Conversion Electron Intensity[a,b]		
	K_{e-}	$\sum L_{e-}$	$\sum (M+N)_{e-}$
1693.7	≈ 1.2	1.4	
1696.6	10.4		
1704.7	2.0	⩽ 0.6	
1722.0	2.0		
1765.8 + 1768.2	0.81 (20)		
1774.6	3.0 (5)	0.3	
1820.0	0.4 (1)		
1823.7	7.5 (1.3)	0.8 (3)	
1862.7	6.4 (1.1)	0.84 (17)	0.3
1949.8	0.21 (05)		
1956.5	1.0 (2)		
1977.9	0.88 (20)		
2044.8	1.3 (4)		
2192.3	0.10 (4)		
2219.5	0.17 (6)		
2307.7	0.15 (5)		
2317.1	0.11 (4)		
2405.3	0.23 (10)		
2832.0	0.39 (22)	⩽ 0.07	
2920.4	0.16 (9)		

(continued)

Table II. Continued

[a]Except as otherwise indicated, relative intensity errors may be taken to be ≈ 15%. These errors reflect the combined systematic uncertainties arising from the following: 1) normalization to the 710.5-keV K-conversion line; 2) the efficiency of the Si(Li) device and of the Ge(Li) detector used to determine the Si(Li) e^- detection efficiency by the method described in Ref. 8.

[b]Intensities marked with a (†) are from Ref. 2, normalized to the 201.8-keV K-conversion line.

Table III. Relative Intensity of γ-rays from decay of ^{176m}Lu to levels in ^{176}Hf.

E_γ (keV)	Relative Intensity	^{176}Hf Level Assignment
88.35	$(1.2 \pm 0.2) \times 10^6$	88.35
201.8†	[11]†	290.2
936.4	13 ± 2	1226.6
957.4	2.0 ± 0.4	1247.7
1061.6	54 ± 5	1149.9
1138.3	15 ± 2	1226.6
1159.3	100 ± 8	1247.7
1204.8	6.0 ± 1.0	1293.2
1226.7	8.6 ± 1.2	1226.6
1247.7	1.1 ± 0.3	1247.7

†Obscured by ^{177}Lu lines. Intensity derived from 936.4- and 957.4-keV intensities and theoretical conversion coefficient for 202-keV transition.

Table IV. Derived values of the E0-E2 branching parameter, $X = \frac{\rho^2 R_o^4 e^2 (I_n' 200 | I_1' 0)}{B(E2)}$, for decay of K=0+ states in ^{176}Hf.

$\frac{I_n\pi \xrightarrow{e^-} I_1\pi}{I_n'\pi \xrightarrow{\gamma} I_1'\pi}$	$\frac{E_{e^-}(\text{keV})}{E_\gamma(\text{keV})}$	$\frac{\text{Int. } e_K^-}{\text{Int. } \gamma}$	$X = \frac{B(E0)}{B(E2)}$
$\frac{0_2^+ \xrightarrow{e^-} 0_1^+}{0_2^+ \xrightarrow{\gamma} 2_1^+}$	$\frac{1150}{1062}$	$\frac{0.091\ (14)}{10.0\ (9)}$	0.17 ± 0.03
$\frac{2_2^+ \xrightarrow{e^-} 2_1^+}{2_2^+ \xrightarrow{\gamma} 2_1^+}$	$\frac{1138}{1138}$	$\frac{0.34\ (5)}{12.6\ (1.0)}$	0.19 ± 0.04[a]
$\frac{2_2^+ \xrightarrow{e^-} 2_1^+}{2_2^+ \xrightarrow{\gamma} 0_1^+}$	$\frac{1138}{1227}$	$\frac{0.34\ (5)}{6.8\ (9)}$	0.35 ± 0.07[a]
$\frac{2_2^+ \xrightarrow{e^-} 2_1^+}{2_2^+ \xrightarrow{\gamma} 4_1^+}$	$\frac{1138}{936}$	$\frac{0.34\ (5)}{10.4\ (8)}$	0.15 ± 0.03[a]
$\frac{0_3^+ \xrightarrow{e^-} 0_1^+}{0_3^+ \xrightarrow{\gamma} 2_1^+}$	$\frac{1293}{1205}$	$\frac{1.58\ (24)}{6.1\ (5)}$	8.3 ± 1.3
$\frac{2_3^+ \xrightarrow{e^-} 2_1^+}{2_3^+ \xrightarrow{\gamma} 2_1^+}$	$\frac{1291}{1291}$	$\frac{\approx 0.39}{24.6}$	(≈ 0.16)[a,b]
$\frac{2_3^+ \xrightarrow{e^-} 2_1^+}{2_3^+ \xrightarrow{\gamma} 0_1^+}$	$\frac{1291}{1379}$	$\frac{\approx 0.39}{(1.0)}$	(≈ 5.6)[a,b]
$\frac{2_3^+ \xrightarrow{e^-} 2_1^+}{2_3^+ \xrightarrow{\gamma} 4_1^+}$	$\frac{1291}{1089}$	$\frac{\approx 0.39}{3.7}$	(≈ 11)[a,b]

(continued)

Table IV. Continued

[a] $\Delta I = 0$, $(2'+ \rightarrow 2+)$ transition assumed to be pure E2. Experimental K-conversion coefficient corrected by using theoretical α_K^{E2} from Ref. 10.

[b] The assignments of the 1379.3-keV γ-ray and K = 0 to the 1379.4-keV level are not confirmed.

FIGURE CAPTIONS

Fig. 1. The Compton-suppressed Ge(Li) γ-ray singles spectrum of ^{176}Ta in the region 80-1245 keV.

Fig. 2. The Compton-suppressed Ge(Li) γ-ray singles spectrum of ^{176}Ta in the region 1060-3000 keV.

Fig. 3. The γ-ray spectra of ^{176}Ta in coincidence with the 88-keV (top) and 202-keV (bottom) ground rotational band transitions in ^{176}Hf.

Fig. 4. The γ-ray spectra of ^{176}Ta in coincidence with the multiplet at 1159 keV. The three spectra shown correspond to adjacent windows set at about 1155 (top), 1157 (middle), and 1159 (bottom) keV.

Fig. 5. Conversion-electron spectrum from decay of ^{176}Ta in the region 160-1620 keV. Taken with a 1-cm^2 × 3 mm deep Si(Li) detector. Unless otherwise noted, peaks are K-shell conversion lines corresponding to the indicated photon transition energy.

Fig. 6. The high-energy electron spectrum of ^{176}Ta (1-3 MeV). Labeling of the peaks is consistent with that of Fig. 5.

Fig. 7. The decay of ^{176}Ta, ^{176}Lu, and ^{176m}Lu to levels in ^{176}Hf.

Fig. 8. The level scheme of ^{176}Hf showing additional transitions observed in ^{176}Ta decay which could be placed on the basis of energy sums and differences alone.

Fig. 9. Computer fits to the ^{176}Ta γ-ray multiplet at 1225 keV, showing the presence of three components.

Fig. 10. The low-energy γ-ray singles spectrum of ^{176}Ta taken with the 1-cm^3 "thin-window" Ge(Li) diode (0-270 keV).

Fig. 11. Computer fit to the ^{176}Ta conversion-electron spectrum in the region about 1290 keV.

Fig. 12. Plot of the theoretical K-conversion coefficients for hafnium (Z=72) from Hager and Seltzer (Ref. 10). The E3 K-conversion coefficients parallel the values for M1 transitions rather closely for the region of interest above 150 keV.

Fig. 13. The (511 + 512)-keV coincidence spectrum from ^{176}Ta decay (90°).

Fig. 14. High energy γ-ray singles spectrum from ^{176m}Lu decay.

Fig. 15. Comparison of ^{176}Hf levels with theory from Bes,[24,25] Malov and Soloviev,[26] Mikoshiba *et al.*,[28] and Neergård and Vogel.[27]

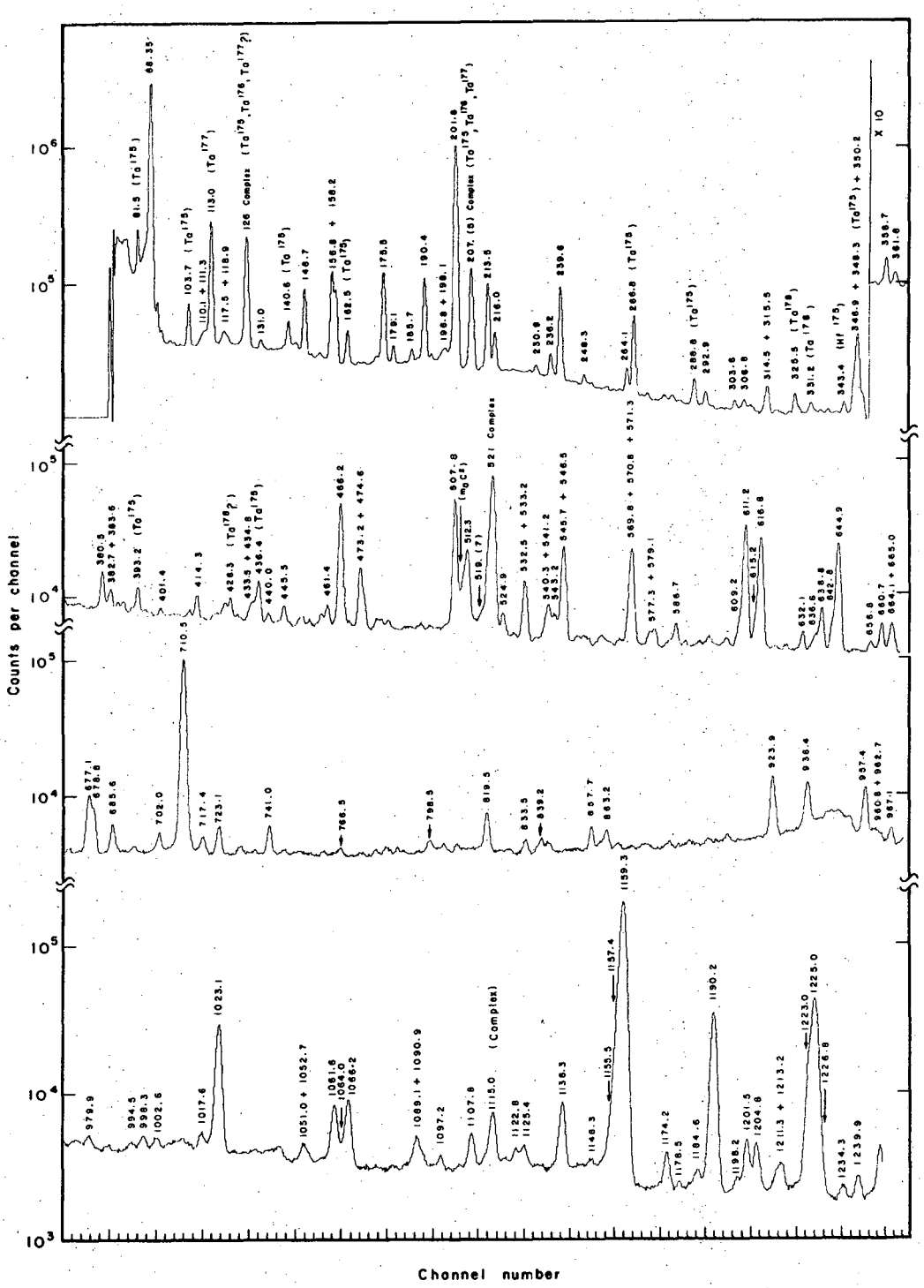

Fig. 1

XBL706-3077

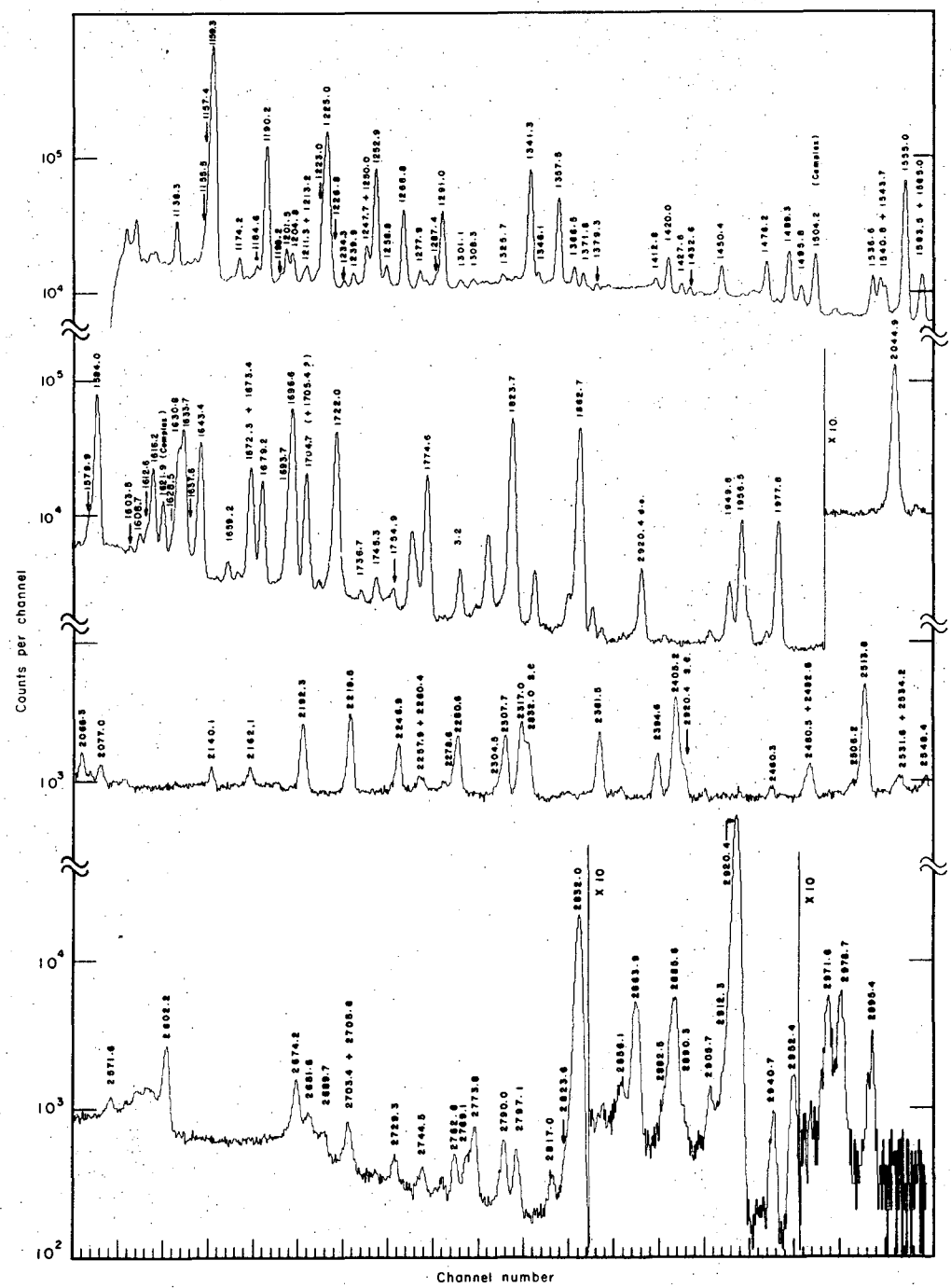

XBL706-3078

Fig. 2

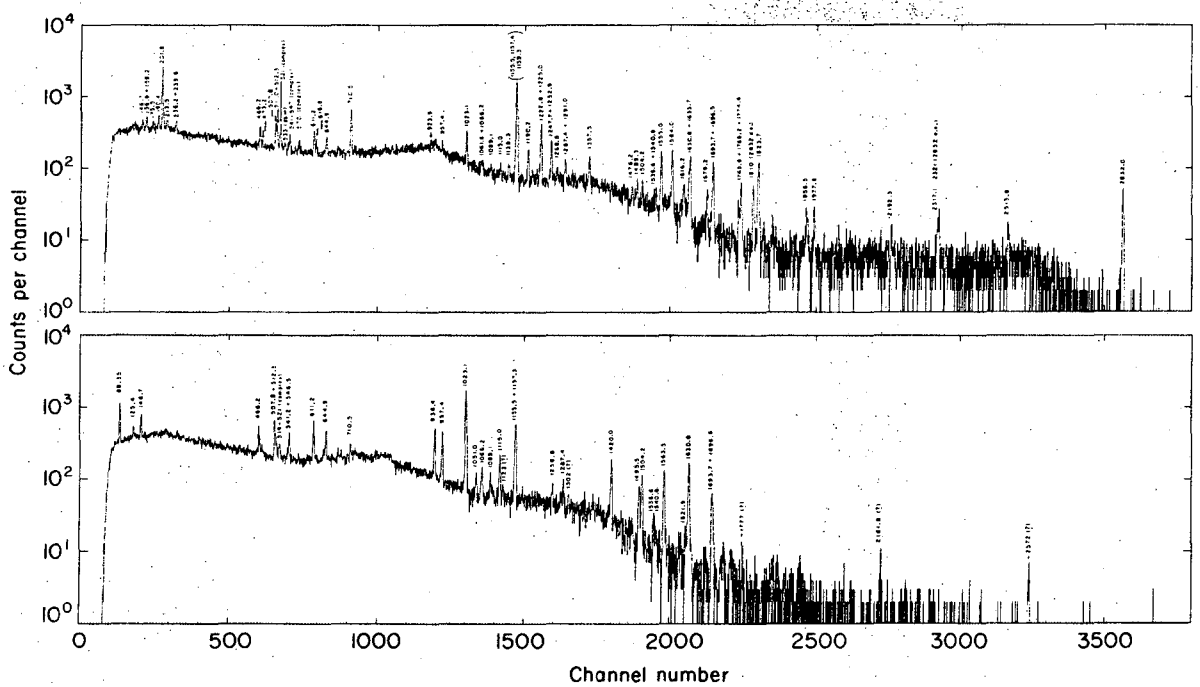
Counts per channel
Channel number
0
500
1000
1500
2000
2500
3000
3500
XBL706-3081

Fig. 3

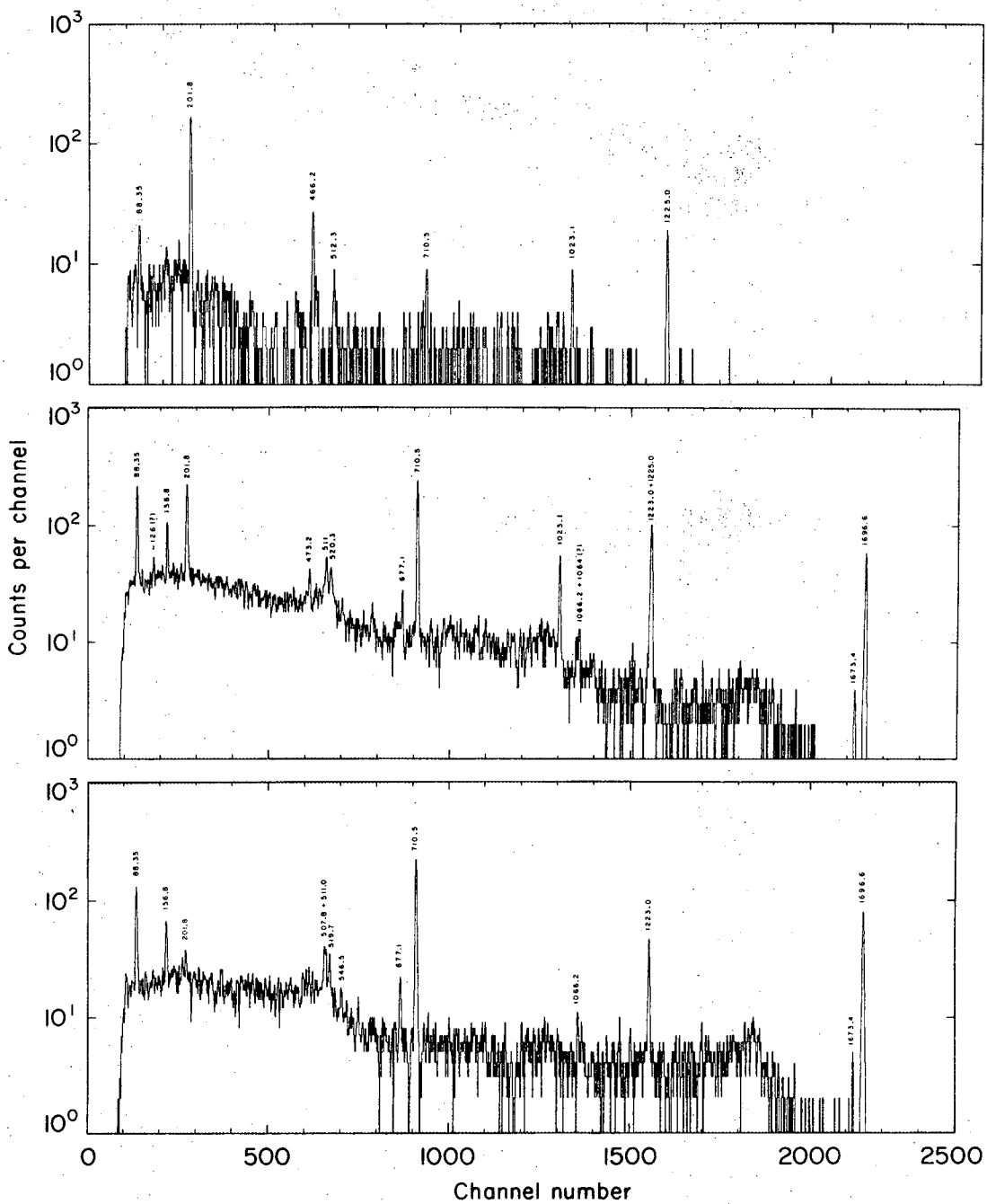

XBL706-3076

Fig. 4

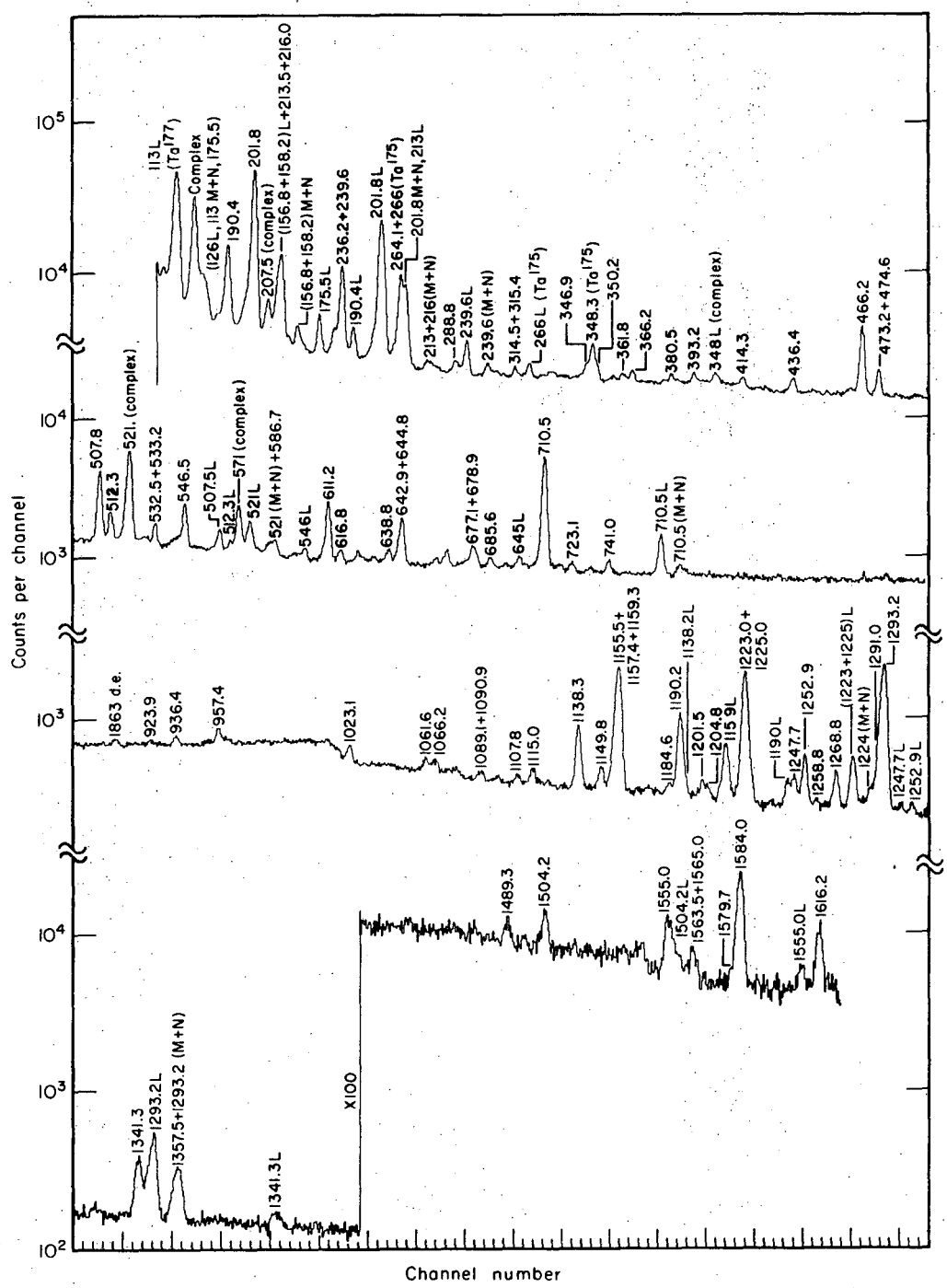

XBL706-3080

Fig. 5

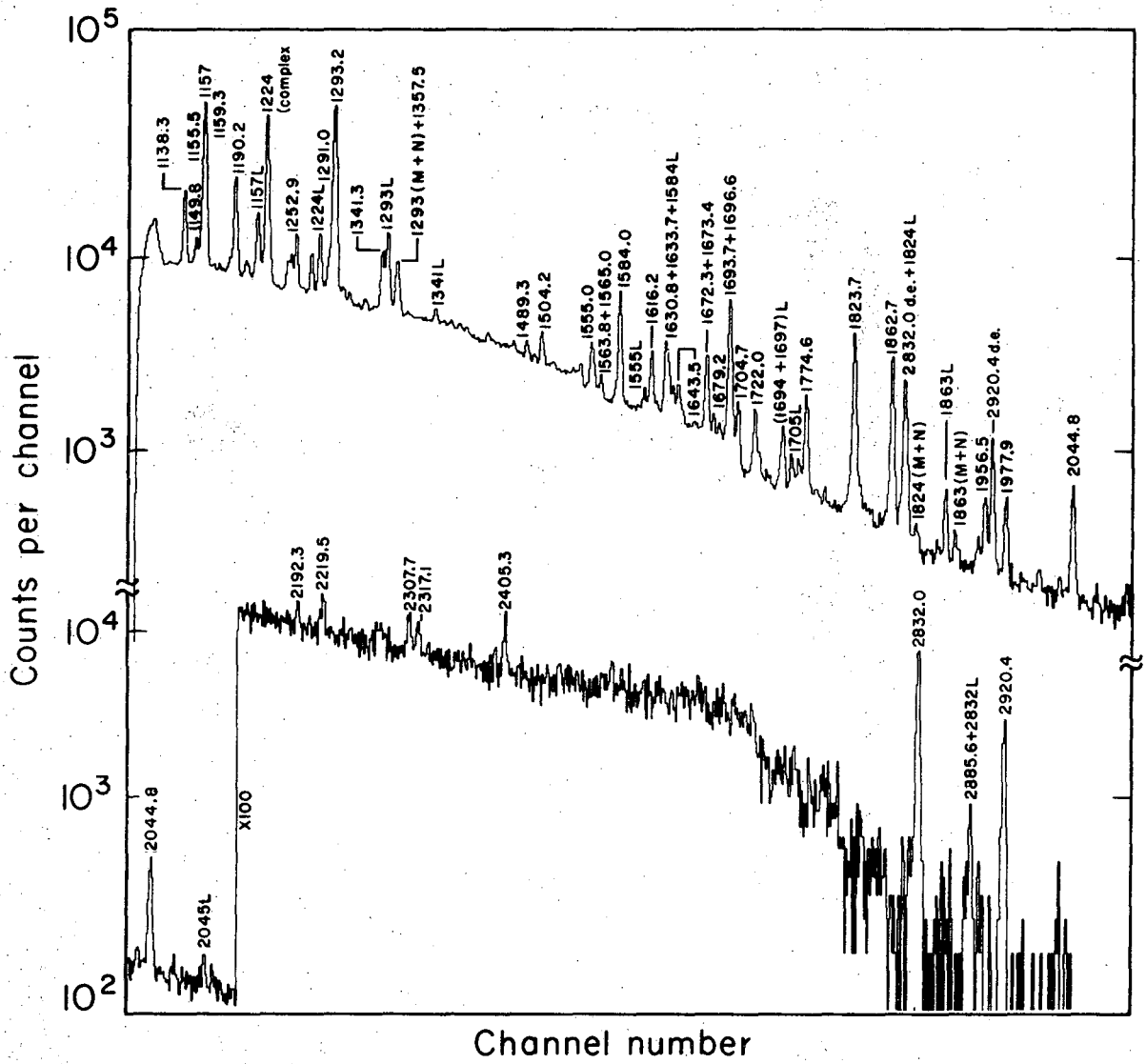

XBL706-3073

Fig. 6

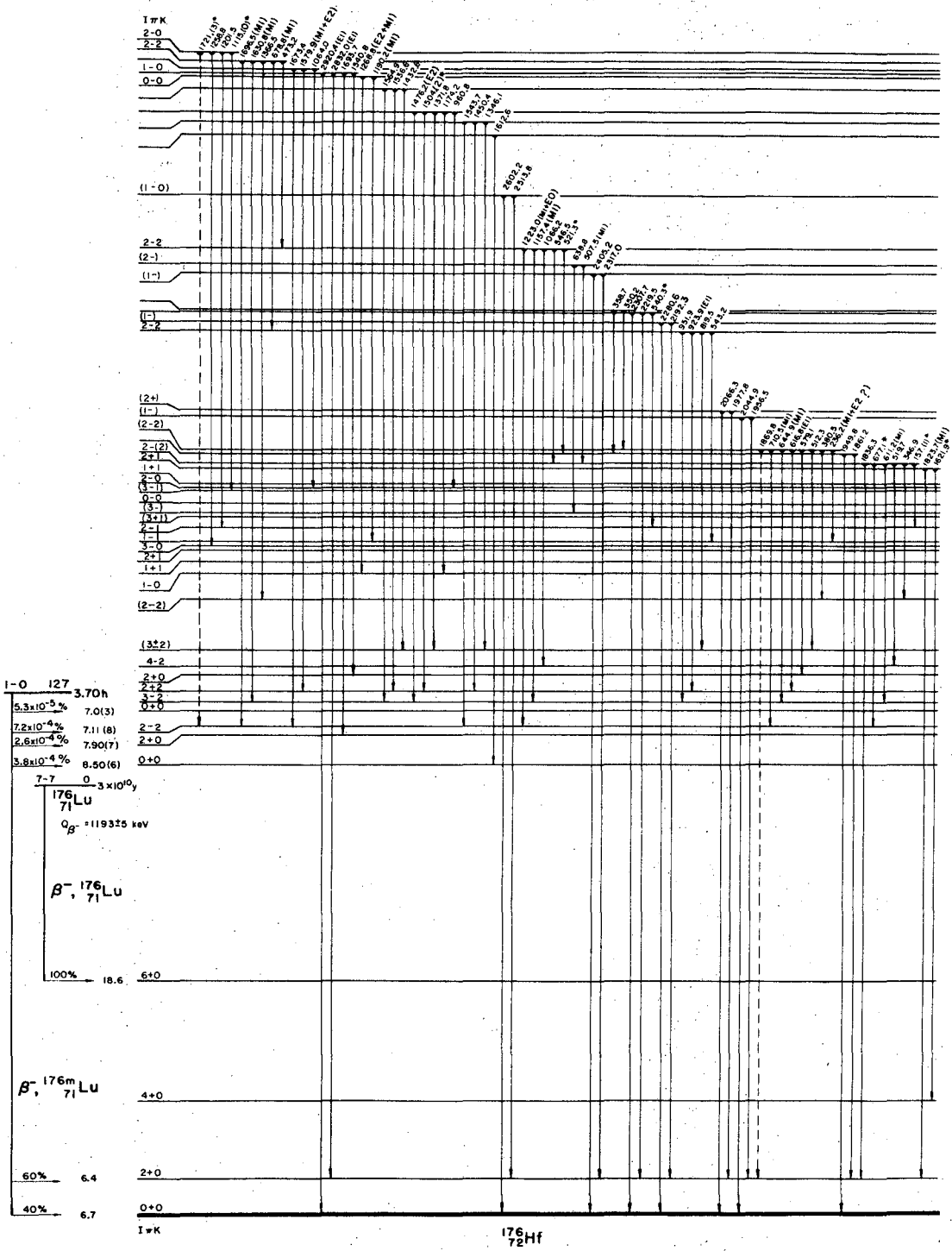

XBL 707-1666

Fig. 7

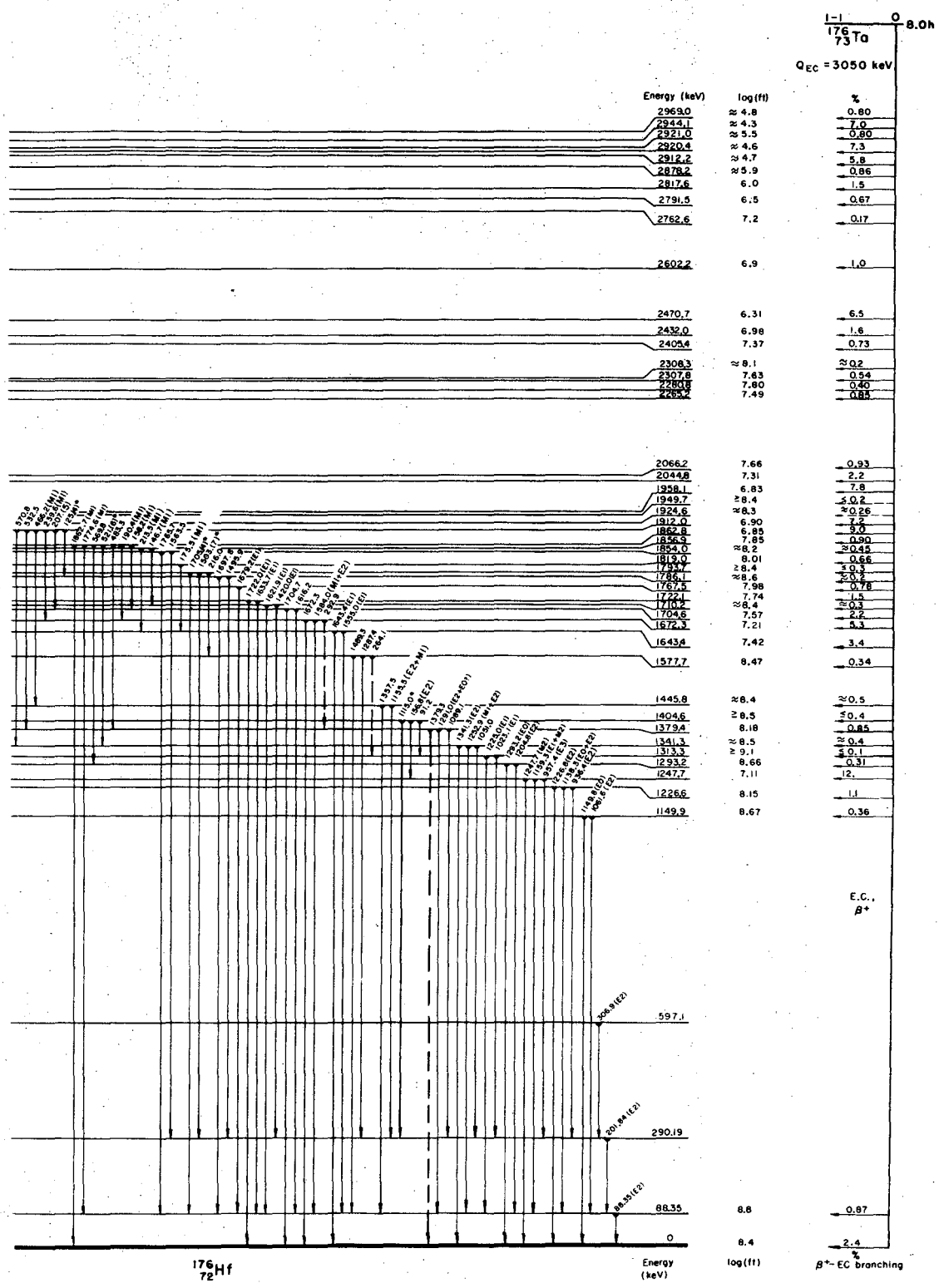
1-1
0
8.0h
176 73Ta
Q_EC = 3050 keV
Energy (keV)
log(ft)
%
2969.0
2944.1
2921.0
2920.4
2912.2
2878.2
2817.6
2791.5
2762.6
2602.2
2470.7
2432.0
2405.4
2306.3
2307.8
2280.8
2265.2
2066.2
2044.8
1958.1
1949.7
1924.6
1912.0
1862.8
1856.3
1854.0
1819.0
1793.7
1786.1
1767.5
1722.1
1710.2
1704.6
1672.3
1643.6
1577.7
1445.8
1404.6
1379.4
1341.3
1313.3
1293.2
1247.7
1226.6
1149.9
597.1
290.19
88.35
0
Energy (keV)
log(ft)
β+- EC branching
E.C., β+
176 72Hf
XBL 706-3074

Fig. 7 cont.

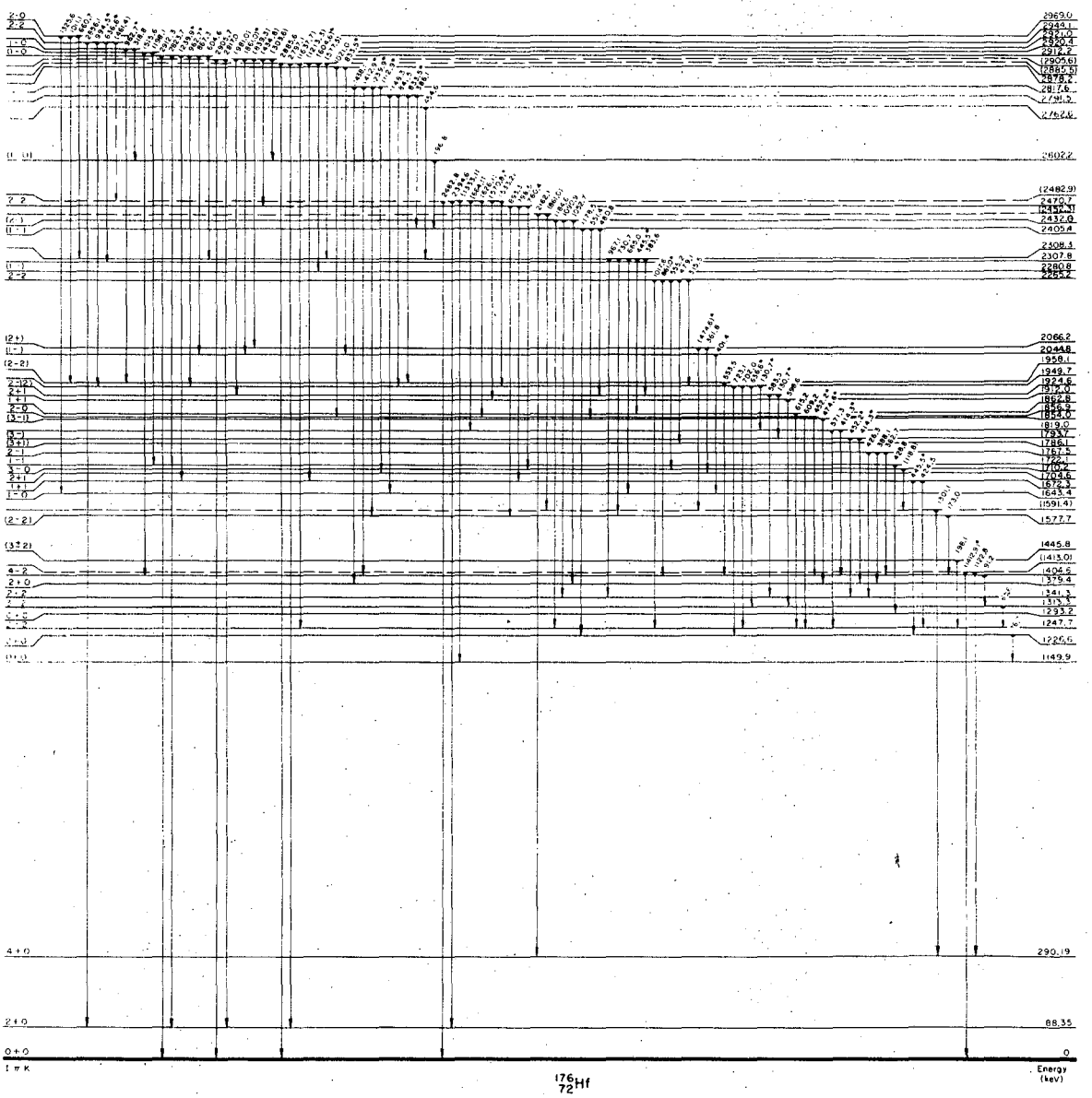

Fig. 8

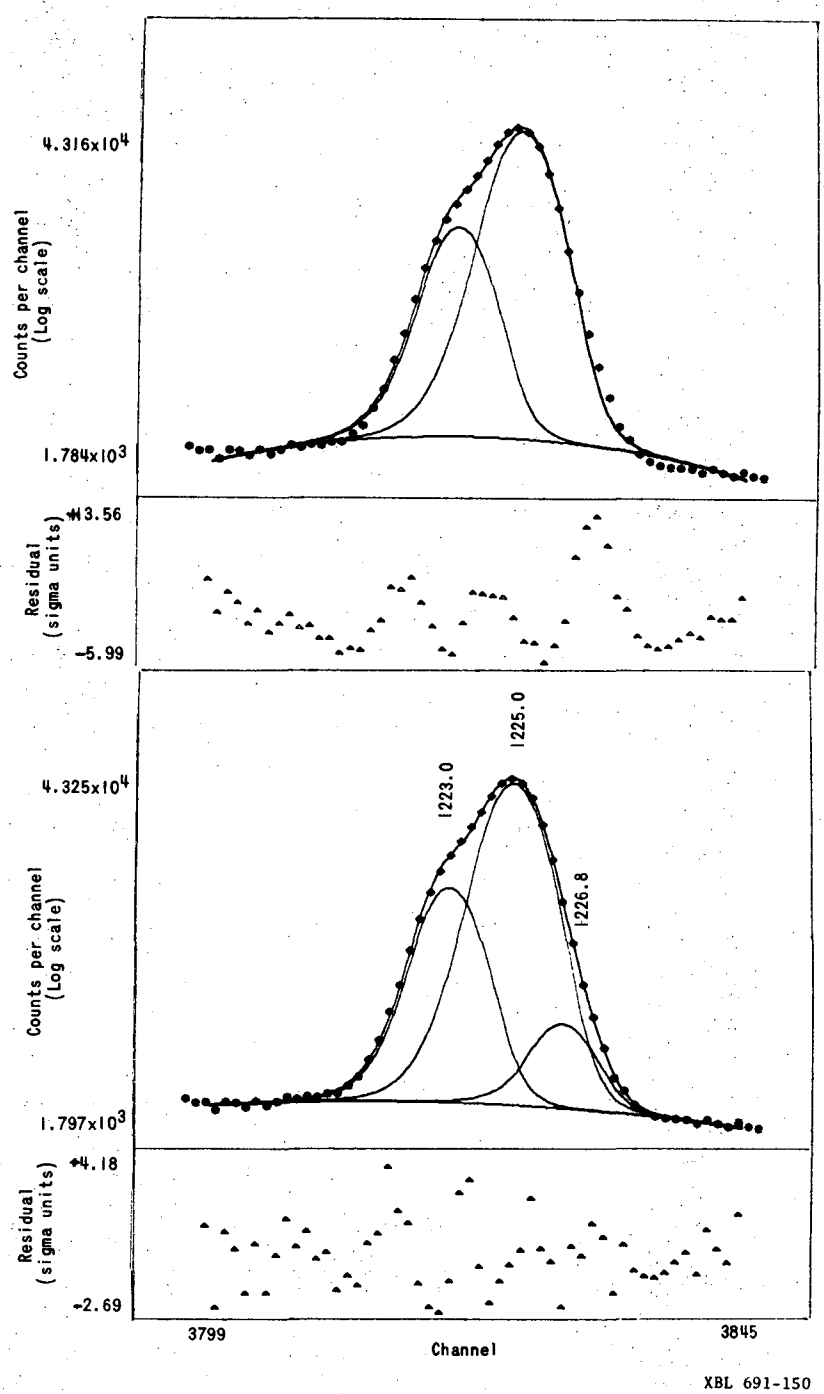
4.316x10^4
Counts per channel (Log scale)
1.784x10^3
+3.56
Residual (sigma units)
-5.99
1225.0
1223.0
1226.8
4.325x10^4
Counts per channel (Log scale)
1.797x10^3
+4.18
Residual (sigma units)
-2.69
3799
3845
Channel
XBL 691-150

Fig. 9

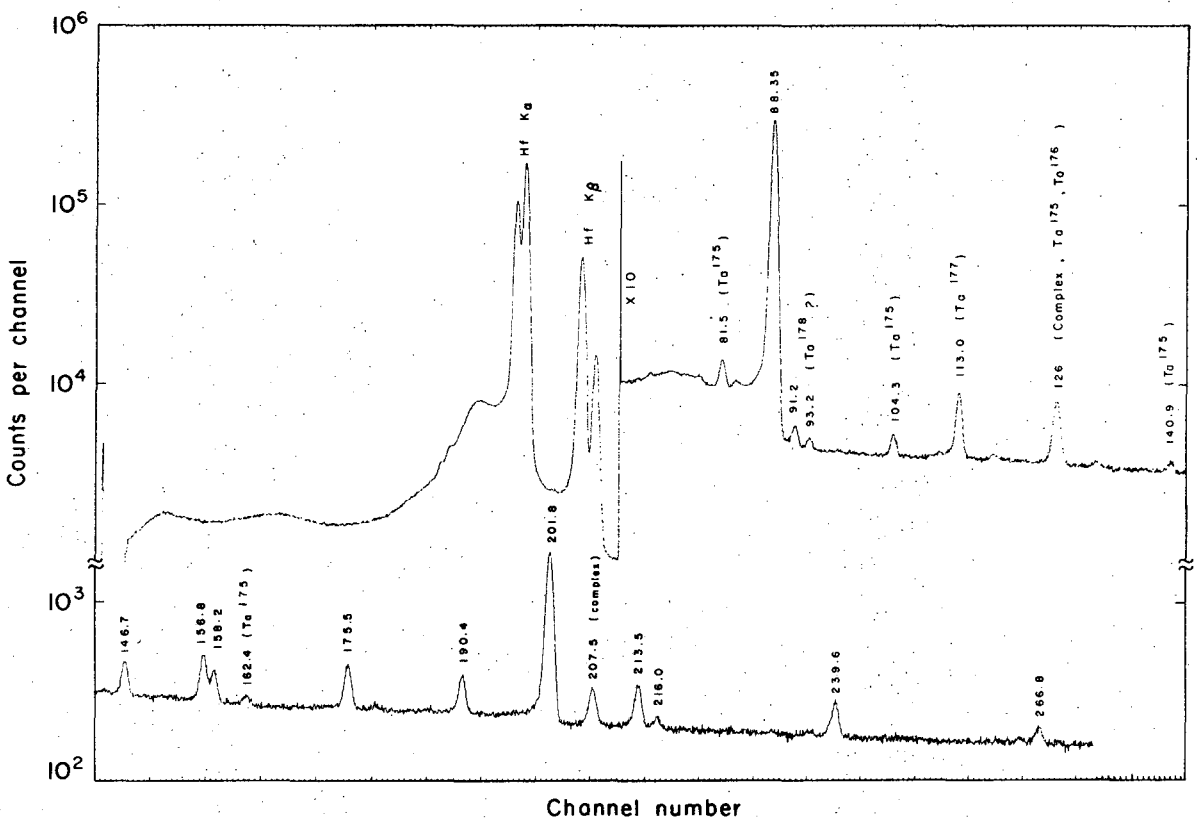

XBL706-3075

Fig. 10

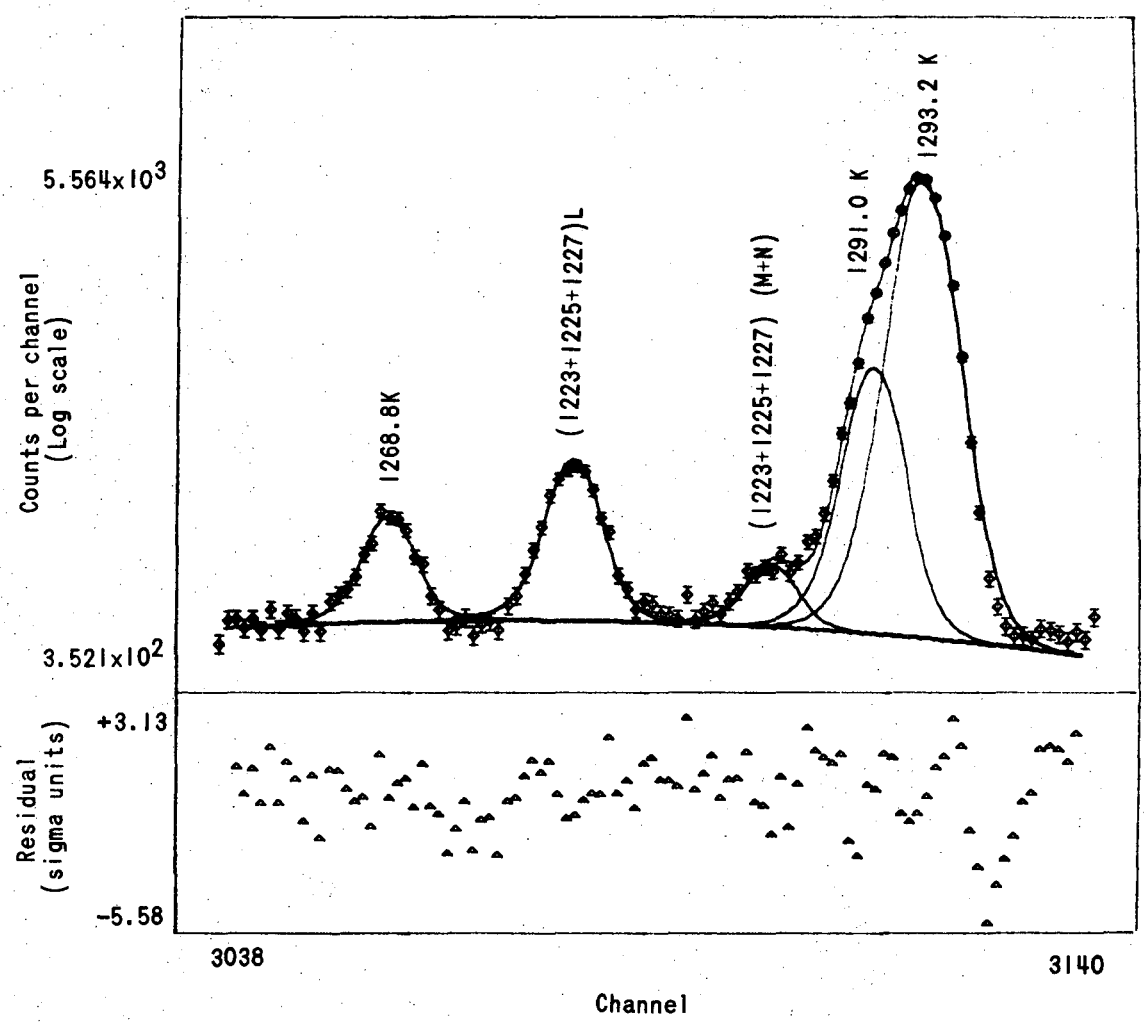

XBL 691-142

Fig. 11

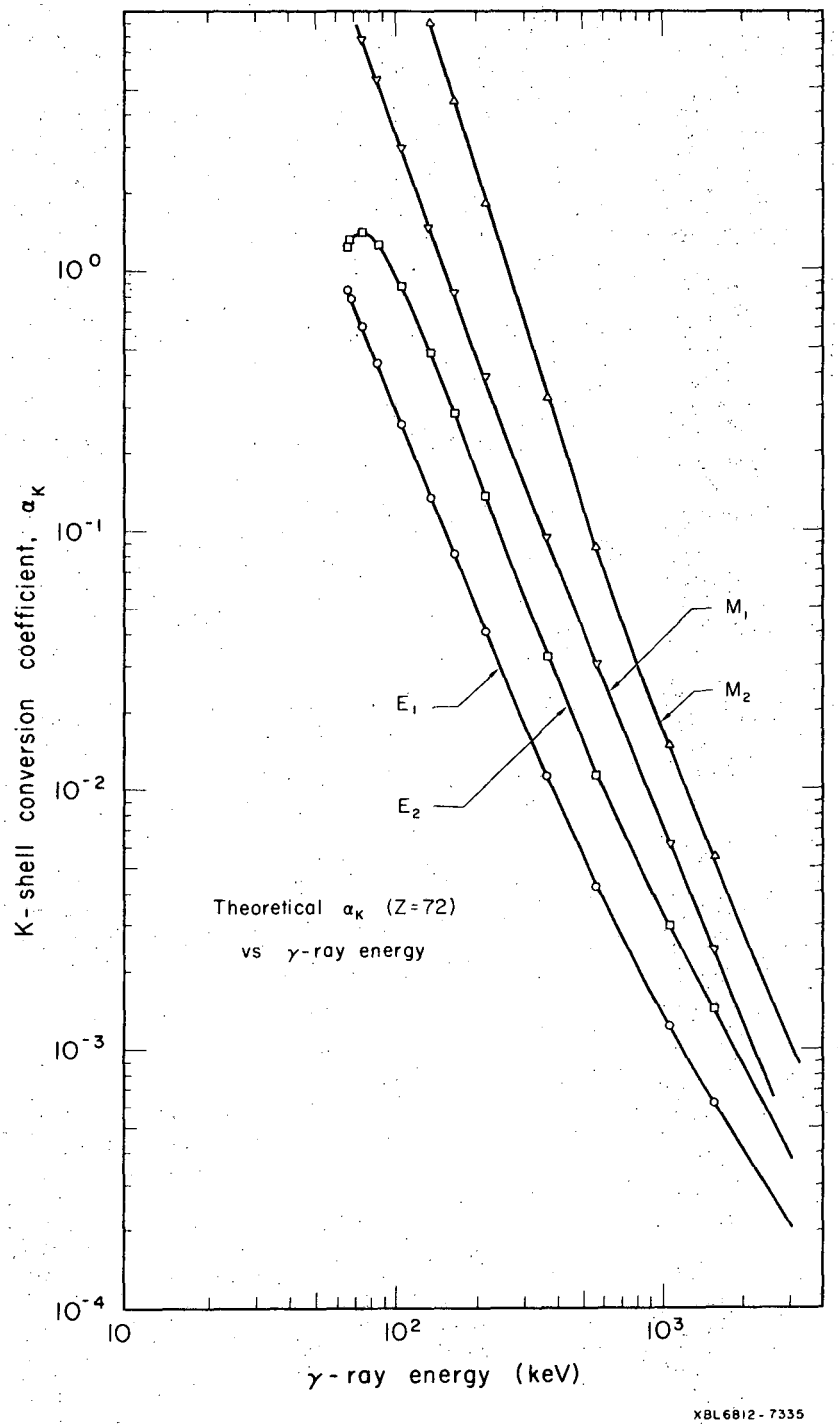
K-shell conversion coefficient, α_K
10^0
10^{-1}
10^{-2}
10^{-3}
10^{-4}
10
10^2
10^3
γ-ray energy (keV)
M_1
M_2
E_1
E_2
Theoretical α_K (Z=72)
vs γ-ray energy
XBL6812-7335

Fig. 12

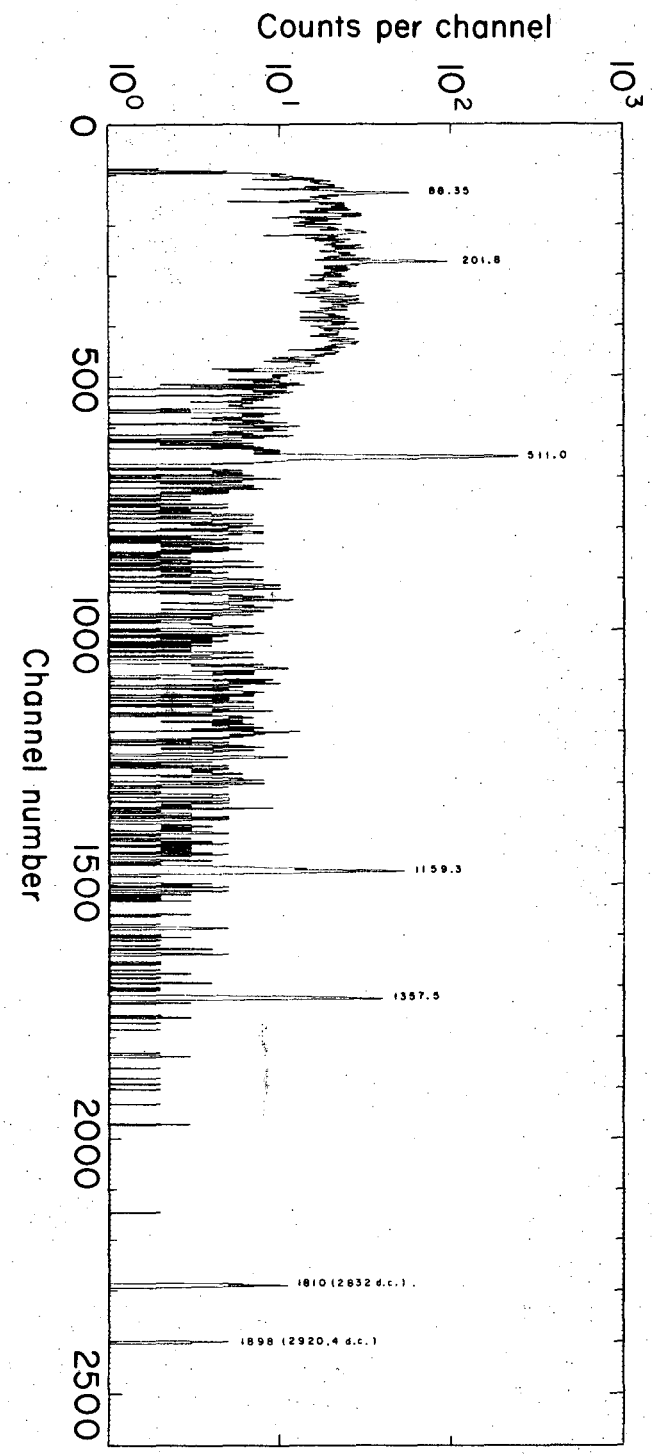
Counts per channel
10^0
10_1
10^2
10^3
0
500
1000
1500
2000
2500
Channel number
88.35
201.8
511.0
1159.3
1357.5
1810 (2832 d.c.)
1898 (2920.4 d.c.)
XBL706-3079

Fig. 13

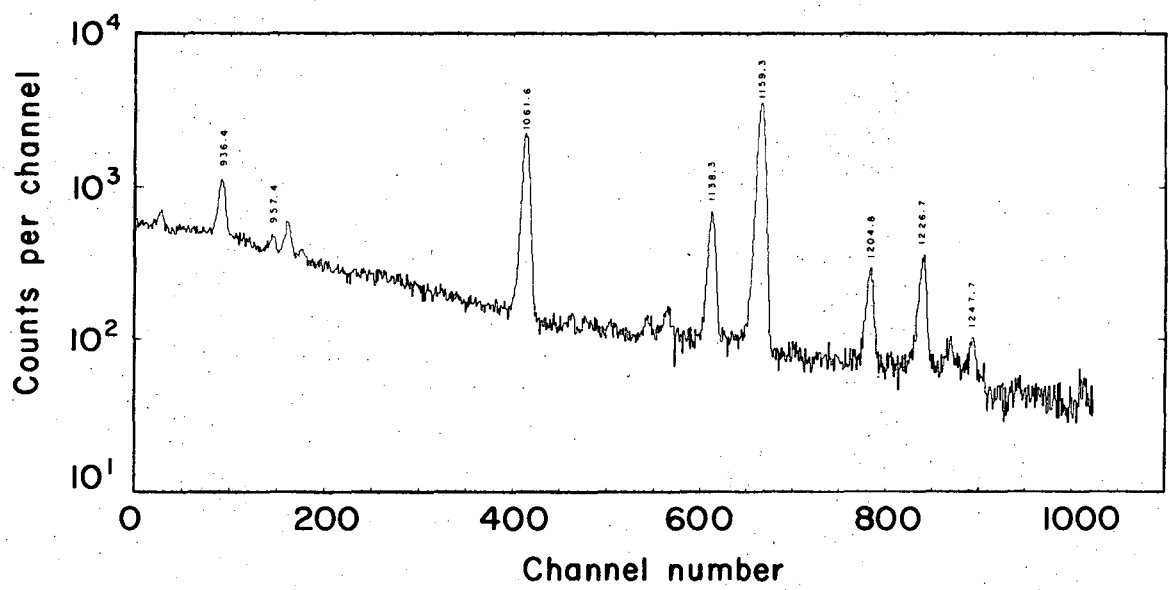

XBL706-3082

Fig. 14

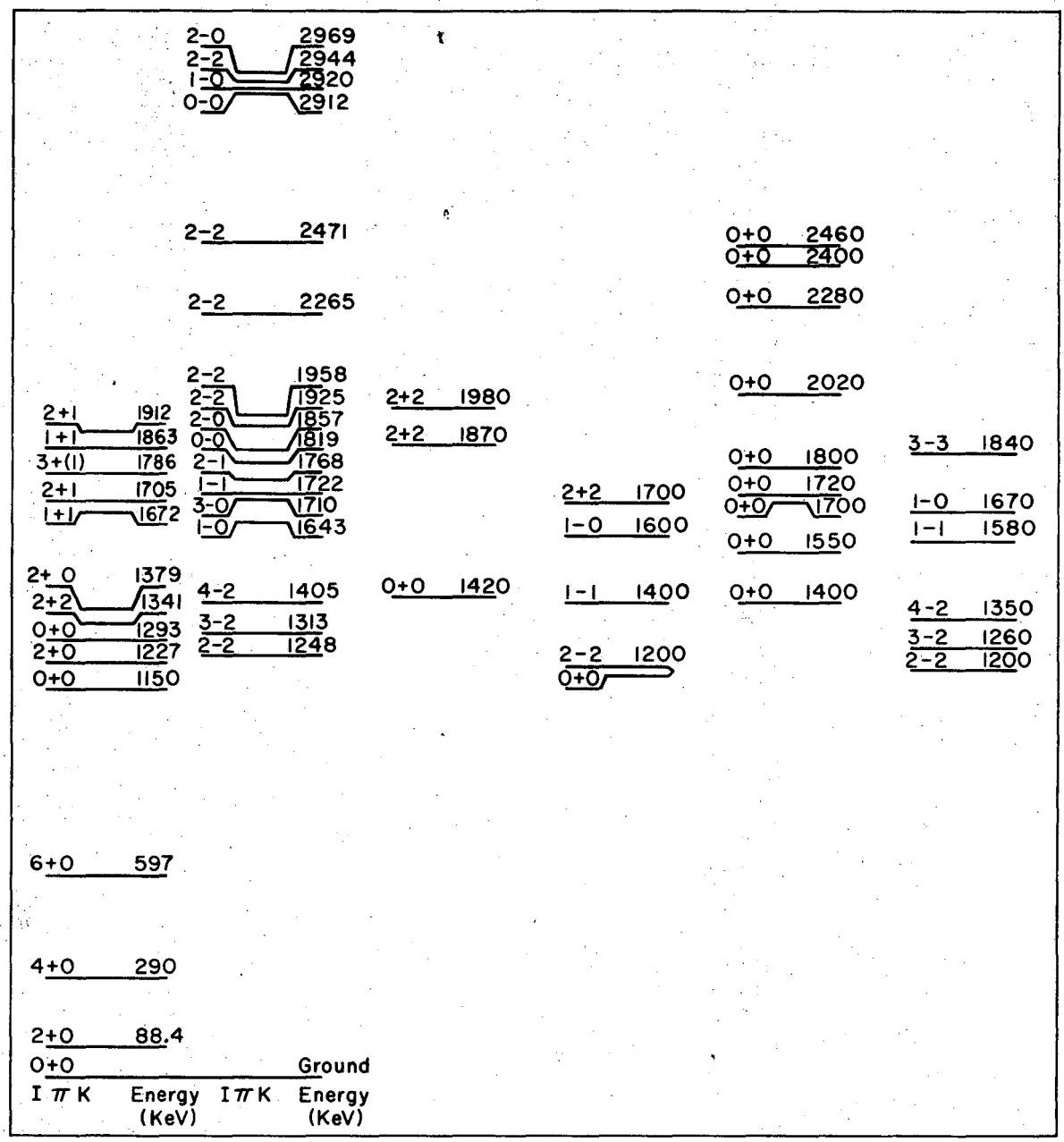

XBL-704-2688

Fig. 15

TECHNICAL INFORMATION DIVISION
LAWRENCE RADIATION LABORATORY
UNIVERSITY OF CALIFORNIA
BERKELEY, CALIFORNIA 94720